Research Article

Ru Li, Sen Li*, Yuanhao Wang, and Hongyi Shen

Application of iron-based catalysts in the microwave treatment of environmental pollutants

https://doi.org/10.1515/gps-2025-0060
received March 16, 2025; accepted August 21, 2025

Abstract: The existence of various pollutants in the environment threatens the health of nature and mankind. Microwave (MW) catalysis, an emerging technology featuring rapid reaction rates, uniform heating, energy-saving efficiency, and environmental friendliness, is expected to fill the gaps in existing catalytic treatment technologies. Iron-based catalysts, which are abundantly distributed, economically sustainable, and possess excellent composite magnetic permeability and electromagnetic wave-absorbing properties, show great potential in MW catalysis. This review classifies iron-based catalysts for MW catalysis and investigates their interactions with MWs. Additionally, various characterization techniques are used to analyze the structural and compositional features of these catalysts. The correlation between the performance, structural morphology, and chemical composition of Fe-based is systematically discussed. The reaction devices, treatment objects, and parameters that influence the use of iron-based catalysts to treat environmental pollutants under MW irradiation are introduced. The application of density functional theory in treating environmental contaminants with iron-based catalysts under MW irradiation and the technological means to enhance the coupling of MW catalysis are described. Finally, future research prospects are proposed.

Keywords: microwave, iron-based catalysts, environmental pollutants, DFT

*** Corresponding author: Sen Li,** School of Geography and Environmental Sciences, Guizhou Normal University, Guiyang, 550000, China; Guizhou Normal University National Key Laboratory Breeding Base of Karst Mountain Ecological Environment in Guizhou Province, Guiyang, 550000, China; Center of R&D, Guizhou Merit Environmental Technology Co., Ltd, Guiyang, 550000, China,
e-mail: 201912005@gznu.edu.cn, tel: +86 185 8581 1471
Ru Li: School of Geography and Environmental Sciences, Guizhou Normal University, Guiyang, 550000, China; Guizhou Normal University National Key Laboratory Breeding Base of Karst Mountain Ecological Environment in Guizhou Province, Guiyang, 550000, China,
e-mail: 1847123207@qq.com
Yuanhao Wang: Hoffmann Institute of Advanced Materials, Shenzhen Polytechnic, Shenzhen, 518055, China
Hongyi Shen: Guizhou Wantong Environmental Protection Engineering Co., Ltd, Guiyang, 550000, China

1 Introduction

With the diversification of natural succession and human activities, various pollutants enter the atmosphere, water, soil, and other environments through different pathways, threatening the health of humans and other living things. For example, heavy metals, dyes, pesticides, antibiotics, medical waste, phenols, and many other pollutants all exhibit persistent toxicity and mutagenicity [1–7]. To solve the above environmental pollution problems, treatment methods such as adsorption, photocatalysis, membrane separation, electrocatalysis, biological process, Fenton reaction, etc., have appeared, but all of them have different degrees of limitations, such as being prone to secondary pollution, inefficiency, low stability, high treatment cost, high energy consumption, long time-consuming, and narrow pH range [1,8–18]. Therefore, there is a need to find more promising ways to treat pollutants. Microwave (MW) catalysis, as an emerging technology, has the potential to fill a gap in current catalytic technology, gradually attracting the attention of researchers.

MW is electromagnetic radiation in the free-space wavelength λ range from 1 m (frequency f = 300 MHz) to 1 mm (frequency f = 300 GHz) [19]. MW heating is an electromagnetic radiation technology with several advantages, such as rapid and uniform heating, low energy consumption, and selective heating [20,21]. To prevent interference with the specified wide range of frequencies in the telecommunications industry, only frequencies around 2.45 GHz are allowed for MW heating reactions. Before the use of MW heating, high-frequency induction heating methods were generally used. It was not until 1946, when Percy Spencer was passing an open radar and a bar of

chocolate in his pocket melted, that he thought there might be some connection between MW radiation and food, and Raytheon invented the first patented commercial MW furnace [22]. In addition to being closely related to food, MW radiation is commonly used in the preparation of materials in the laboratory and various catalytic reaction processes, in which MW-assisted catalysis mainly interacts with catalysts. Under MW irradiation, the catalyst surface produces a "hot spot" effect, and then a series of reactions occur to decompose the contaminated matter [23]. MW catalysis technology is significantly more efficient at treating contaminants in the environment than using catalysts alone or MW irradiation. Ideal MW catalysts should have a large specific surface area, a crystalline nature, room-temperature ferromagnetism, good dielectric characteristics, and structural stability even at high temperatures [24]. Common MW catalysts include carbon-based catalysts, iron-based catalysts, and others, among which iron-based catalysts have some advantages, such as economic sustainability, and are widely used in MW catalysis.

Iron is a transition metal with lower toxicity than copper and manganese, and Fe-based catalysts are low-cost, environmentally friendly, sustainable, and widely distributed in large quantities [25–27]. In the field of MW-induced catalysis technology, the kinetics and pathways of catalytic reactions are altered by introducing MW energy, which is more efficient and energy-saving. MW can produce heat in the medium, improving the catalytic ability of iron-based catalysts through "hot spots" [21]. In 2005, Oh et al. were the first to complete kinetic experiments on the reduction of perchlorate by iron using MW heating and conventional heating. The results confirmed that iron under MW irradiation can have a good effect on the transformation of contaminants [28]. In recent years, the types of iron-based catalysts used in combination with MW are more diverse, with hematite, ferrite, and zero-valent iron being involved [29–31].

At present, MW catalysts have been classified in some reviews, such as carbon-based catalysts, iron-based catalysts, and other types mentioned above. However, specific catalysts have not been explored in further detail, and iron-based catalysts for MW catalytic processes are poorly categorized and mechanistically unclear. Based on previous studies, this article summarizes the basic principles of MW heating, introduces Fe-based materials for MW catalysis and their common characterization methods, describes the application of Fe-based catalysts in the treatment of environmental pollutants under MW irradiation, and gives an outlook on future research work.

2 MW heating principle

The MW heating mechanism is mainly divided into thermal effect and non-thermal effect. The thermal effect is when the MW energy is absorbed by the medium material and converted into heat, resulting in an overall or local temperature rise phenomenon [32,33]. When a liquid medium (e.g., water) with a permanent dipole moment is subjected to an alternating electric field (MW radiation), the dipoles rotate at high frequency in the direction of the electric field, and the rapid translational motion of the particles induces "internal friction" and is converted into thermal energy. Unlike conventional heat dissipation from the surface to the center of a material by conduction, convection, and radiation, MW heating generates heat throughout the entire volume of the material, and rapid "volume heating" occurs, resulting in the internal temperature of the material being higher than the external temperature [34]. For solid materials, their interactions with MWs can be categorized into four groups (Figure 1): (1) perfect conductors such as a metal or graphite, which reflect MWs from their surfaces; (2) insulators such as polypropylene or quartz glass, which transmit MWs; (3) dielectric loss materials such as silicon carbide, which absorbs MWs and converts them into heat; and (4) magnetic loss materials such as ferrite, which incur magnetic losses in the MW field [22].

Non-thermal effects refer to chemical, physical, or biochemical changes in a material induced by MWs when the system temperature is kept constant [35,36]. They are produced when the polarized portion of the material is aligned with the electric poles of the electric field, which can lead to the excitation of reactant molecules to high rotational and vibrational energies, resulting in the weakening of polar bonds, the promotion of high-frequency oscillations of polar molecules weakening the strength of the chemical bonding, and the lowering of the activation energy of the reaction, intensifying the transfer of electrons, and enhancing the exposure of the active sites, resulting in the degradation of the pollutant molecules [37–41]. Ren et al. found that MWs not only acted as a heat source in the Fe/Cu bimetallic system but also enhanced the pollutant removal efficiency by strengthening the electron transfer, exposing the active sites, accelerating the mass transfer, and other non-thermal effects through the heated-Fe/Cu and MW-Fe/Cu systems in controlled experiments [42]. Yuan et al.'s study found that the non-thermal effects generated by MW radiation could enhance the efficiency of pollutant removal by increasing the internal energy of NO molecules, weakening the N–O bond, and exciting polar NO

into excited state NO*, which is conducive to the deep oxidation of NO*, making the catalytic oxidation of NO more rapid and thorough than conventional heating [43].

MW heating relies on the ability of certain materials (e.g., iron-based catalysts) to convert electromagnetic energy into thermal energy, can be expressed in terms of the material's dissipation factor (or tanδ), and is calculated by Eq. 1:

$$\tan \delta = \frac{\varepsilon''}{\varepsilon'} \quad (1)$$

where ε'' is the dielectric loss factor (the imaginary part of the dielectric properties) and ε' is the relative dielectric constant (the real part of the dielectric properties).

When the MW enters the medium, the medium absorbs the MW and converts it into heat, while the field strength and power of the MW gradually attenuate, and there are differences in the absorption and attenuation ability of different media to MW energy. Penetration depth (D) refers to the MW field strength from the surface of the material, attenuation to the surface value of $1/e$ (36.8%) of the distance, which is determined by the complex dielectric constant of the medium, used to represent the medium on the attenuation of MW energy, as shown in Eq. 2:

$$D = \frac{\lambda_0}{\pi \tan \delta \sqrt{\varepsilon'}} \quad (2)$$

where λ_0 is the free-space wavelength, ε' is the relative permittivity, and tan δ is the dielectric loss angle tangent. The penetration depth increases with the wavelength, and since the MW frequency is inversely proportional to the wavelength (the higher the frequency, the shorter the wavelength), the higher the MW frequency, the weaker the penetration ability. For typical media, $\pi \tan \delta \sqrt{\varepsilon'} \approx 1$, MW penetration depth, and wavelength in the same order of magnitude, while the wavelength of infrared heating is usually only a few tens of nanometers, which is much smaller than the MW wavelength. Therefore, MWs have a stronger penetration ability to dielectrics, and they can heat deeply inside the material, which in turn produces various types of heating effects [44].

3 Iron-based materials for MW catalysis

Iron-based catalysts have low coercivity and high magnetic saturation, good composite permeability, and excellent electromagnetic wave absorption ability, and show high removal efficiency for pollutants in MW catalytic systems [45]. This section provides an overview of the basic properties of iron-based catalysts, a brief description of the appropriate synthesis methods (Table 1 and Figure 2), as well as the research progress of these materials in MW catalysis.

3.1 Ferrite and ferrite-based composite catalysts

The properties of materials usually depend on the synthesis method; in the past some time, researchers have explored several ferrite preparation methods, including precipitation, sonochemistry, sol–gel method, electrochemical method,

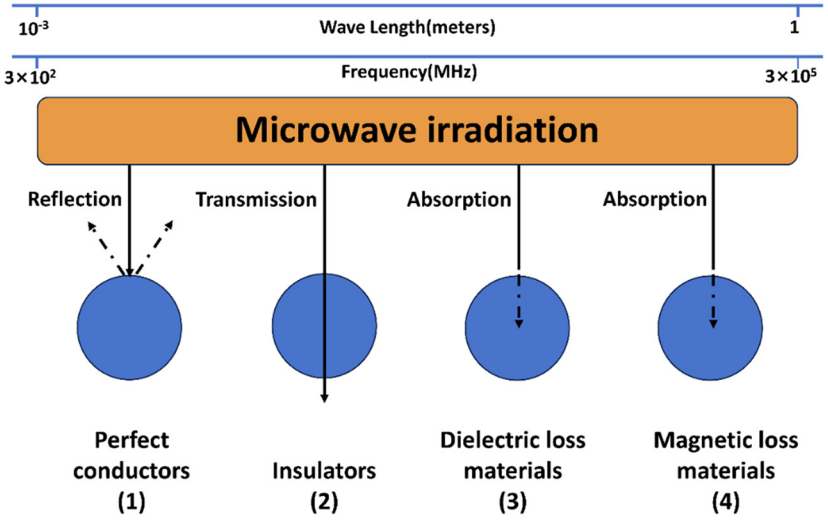

Figure 1: Interaction between MWs and solid samples.

Table 1: Preparation of iron-based catalysts

Type	Catalyst	Synthesis method	Feedstock	Ref.
Ferrite composite catalyst	$Co_{0.5}Zn_{0.5}Fe_2O_4$	Chemical coprecipitation method	$Fe(NO_3)_3{\cdot}9H_2O$, $Co(NO_3)_2{\cdot}6H_2O$	[77]
Ferrite catalyst	$CuFe_2O_4$	MW combustion method	$Cu(NO_3)_2$, $Fe(NO_3)_3$	[78]
Ferrite catalyst	$ZnFe_2O_4$	Solvothermal calcination	$Fe(NO_3)_3{\cdot}9H_2O$, $Zn(CH_3COO)_2{\cdot}2H_2O$	[79]
Ferrite composite catalyst	Mn-Zn ferrite	Nano in situ composite method	$Fe(NO_3)_3{\cdot}9H_2O$, $Mn(NO_3)_2$, $Zn(NO_3)_2{\cdot}6H_2O$	[80]
Ferrite composite catalyst	gCN/$ZnFe_2O_4$/Bi_2S_3 (ZFO/BS)	MW-assisted process	$Bi(NO_3)_3{\cdot}5H_2O$, CH_4N_2S, gCN/$ZnFe_2O_4$	[81]
Zero-valent iron catalyst	BC-nZVI	Pulsed electrodeposition	$Fe_5O_4{\cdot}7H_2O$, thiourea, DBS, biomass activated carbon	[82]
Zero-valent iron catalyst	Mont/nZVI	Liquid phase reduction method	$FeSO_4{\cdot}7H_2O$, montmorillonite, $NaBH_4$	[83]
Zero-valent iron catalyst	NZVI@ZSM5	Homogeneous precipitation	KBH_4, $FeCl_3$, EtOH, ZSM5	[84]
Zero-valent iron catalyst	ZVI@GO	High-energy ball milling method, stirring method, hydrothermal method	$FeSO_4{\cdot}7H_2O$, citric acid, $NaBH_4$, graphene oxide, $(NH_4)_2SO_4$	[85]
Zero-valent iron catalyst	OX-smZVI	Mechanochemical method	ZVI powder, oxalic acid dihydrate	[86]
Iron-based single-atom catalyst	Fe-PANI	impregnation method	Aniline, $(NH_4)_2S_2O_8$, $FeSO_4$, $Fe_2(SO_4)_3$, $FeCl_3$	[87]
Iron-based single-atom catalyst	Fe–N–O	Pyrolysis	$ZnCl_2$, $FeCl_2{\cdot}4H_2O$, $C_8H_6N_4$, oxalic acid dihydrate	[88]
Other iron-based catalysts	Fe–Ni/SiC	MW-sintering method	$Fe(NO_3)_3{\cdot}9H_2O$, SiC, $Ni(NO_3)_2{\cdot}6H_2O$	[89]

Figure 2: Iron-based catalysts for MW catalysis.

template method, microemulsion method, solid-state method, hydrothermal method, and MW radiation. Others, such as ultrasonication, chemical vapor deposition, electrodeposition, pulsed layer deposition, and continuous ion layer adsorption reaction methods, are also popular. The impact of synthesis methods on the characteristics of ferrite materials is discussed, using the usual sol–gel and hydrothermal procedures as illustrations. Other methods are listed in table form.

The sol–gel method forms gels by hydrolysis of metal alcohol salts, and ferritic materials with certain sizes and shapes are mixed by varying a given sol–gel temperature in the range of 25–200°C. With the advantages of solid-state stoichiometric control and the lack of the need to use complex modern instrumentation, it is one of the most widely adopted techniques for controlling microstructure and can be used to synthesize simple ferrite materials [46]. Januskevicius et al. prepared single-phase highly crystalline three-dimensional powders of yttrium-iron chalcocite (YIP), yttrium-iron garnet (YIG), and terbium-iron chalcocite (TIP) using the aqueous sol–gel method using inorganic salts as starting materials, demonstrating the applicability of the method [47]. Furthermore, when researchers compared the magnetic behavior and structure of bismuth ferrate samples made by gel and hydrothermal methods, they discovered that the samples made by the hydrothermal method had clearly defined grains, whereas the samples made by the sol–gel method displayed a non-uniform distribution of grains. Meanwhile, the surface of bismuth ferrite particles can be observed in the hydrothermal method,

which seems to aggregate in a specific direction, and the bismuth ferrite produced by this method has single-phase and crystalline properties, and can also improve the magnetic properties of bismuth ferrite [48]. As we all know, MW absorption performance is closely related to the material's phase composition, which is determined by the chemical composition and technological conditions. Xing et al. synthesized strontium ferrite using the sol–gel process and studied its wave-absorbing characteristics, phase structure, and morphology. The sintering temperature and holding time were found to be closely related to the phase structure, shape, and wave-absorbing properties of the ferrites made by the sol–gel process [49].

However, the sol–gel method presents certain challenges when applied on a large scale, due to the high cost of metal-alcohol salts as raw materials and the time-consuming gelation process, which limits the productivity. In addition, when scaling up from small laboratory trials to industrial scale, it is more difficult to accurately control conditions such as temperature and humidity, and uniformity is difficult to ensure, which limits its scalability to some extent [50]. With the improvement of the process, it is expected to enhance the potential of large-scale application if the cost can be effectively reduced and the process control can be optimized. The hydrothermal method also has similar problems. Although the iron-based catalysts prepared by this method have excellent performance, the reaction needs to be carried out at high temperature and high pressure, which imposes very high requirements on the reaction equipment and a large investment in equipment in the early stage. Moreover, as the volume of the reactor increases, it is difficult to control the uniformity of the internal temperature and pressure distribution, which can easily lead to unstable catalyst quality. However, because it is environmentally friendly (the solvent is mostly water), if breakthroughs can be made in equipment and processes, it still has a large application prospect in future large-scale production.

Shi et al. produced a highly active nano-catalyst of $CdFe_2O_4$ using the hydrothermal method and studied the effect of the catalyst on removing Congo red (CR) under different conditions under MW irradiation. When only MW was irradiated, CR was almost not degraded. When the catalyst was introduced without MW irradiation, the degradation rate of CR was 26.5% after 10 min. Under the condition of 100°C and 700 W output power, the degradation rate of $CdFe_2O_4$ on CR can reach 94.4% after 10 min irradiation with MW, which indicates that $CdFe_2O_4$ was a kind of MW catalyst with excellent performance [51].

In addition, it has been found that modification of ferrite material can improve the material's catalytic activity when exposed to MW irradiation. Zia and his team prepared magnetic $ZnFe_2O_4$ nanoparticles and prepared their nanohybrids using different polycarbazole (PCz) loading amounts. The treatment effect of amoxicillin was evaluated by $ZnFe_2O_4$ and $ZnFe_2O_4$/PCz nanohybrids under MW irradiation, respectively. Among them, the PCz-modified nano-hybrid showed higher degradation efficiency, reaching nearly 99% in 24 min [52].

3.2 Zero-valent iron catalysts

Zero-valent iron (ZVI or Fe^0) is highly reductive and easy to obtain. In particular, nano-zero-valent iron (nZVI), a particle with a particle size of 10–80 nm, is highly active and has a relatively large specific surface area, which makes it an extremely effective catalyst that promotes the release of active substances, thus removing a wide range of pollutants [53]. Nanomaterials can have different catalytic, optical, electronic, chemical, mechanical, and magnetic properties, and their surface area increases significantly with mass, so varying the size of nanomaterials can effectively improve the overall behavior of the particles [54–56]. nZVI particles are prone to agglomeration under the nano effects and their magnetism, and their dispersibility and recyclability are often optimized to improve their applicability. Specific approaches: (I) composite different skeleton matrices, which can solve the dispersion and recycling problems of nZVI to a certain extent, and (II) improve the particle stability and dispersion by surface vulcanization, metal doping, and surface coating [57]. Many methods have been found to produce nZVI catalysts, commonly including mechanical milling, sol–gel, liquid-phase reduction, spray drying, and sonochemistry methods. Among them, the liquid-phase reduction method can prepare nZVI catalysts with small particle size, large specific surface area, and high electron transfer efficiency by adjusting the amount of reductant, reaction temperature, and pH, such as the $NaBH_4$ reduction method, which can produce nZVI with a particle size of <50 nm and a specific surface area of more than 50 $m^2 \cdot g^{-1}$. However, the nZVI prepared by this method is prone to agglomeration, leading to a decrease in activity, and the activity of the nZVI catalysts needs to be improved by surface modification (e.g., CMC, PVC) to improve the dispersion. Mechanical milling method grinds micron-sized iron powder by planetary ball mill to prepare nanoparticles with a wide particle size distribution (50–200 nm), specific surface area of 10–30 $m^2 \cdot g^{-1}$, and high mechanical strength, which is suitable for industrial applications. The sonochemical method uses the

ultrasonic cavitation effect to reduce iron salts, which can promote free radical generation to some extent. Spray-drying method reduces the iron salt solution at high temperature after spray-drying, which is easy to form porous nZVI and can increase the adsorption-catalytic synergy of the catalyst. The sol–gel method forms iron oxide precursors through the sol–gel process and then reduces them to nZVI, which is often combined with a carrier and can regulate the crystal shape. Among them, the mechanical milling method has good potential for industrial application due to its low cost and simple process [58,59].

Combining MW radiation with ZVI or nZVI can effectively remove contaminants. ZVI can induce electron vibration by absorbing MW, and the intermolecular friction can generate heat energy by MW, thereby increasing the temperature of iron molecules and assisting the degradation of pollutants [60,61]. In previous experiments, researchers mostly used nZVI as an absorbing medium to treat contaminated substances. Lee et al. used nZVI combined with 250 MW energy to reduce the activation energy and improve the removal of chlorobenzene in aqueous solution. In the nZVI-aqueous system, when nZVI was used as an electron donor, it oxidized itself at room temperature to form Fe^{2+}, after which Fe^{2+} to Fe^{3+} provided an electron. When nZVI absorbed MW energy, it generated more electrons, which accelerated its oxidation and generated more frictional heat, hence speeding up the reaction [62].

3.3 Iron single-atom catalysts

The catalytically active sites of iron-based single-atom catalysts (Fe-SACs) exist in the form of isolated single atoms, showing excellent selectivity and catalytic activity [63,64]. Single-atom bonding in SACs is elementally unique, and the electronic structure of the single atoms can be controlled using a variety of ways [65]. In the actual preparation procedure, it has been difficult to prevent individual atoms from agglomerating and keep them dispersed. The high cost of preparing SACs using physical deposition methods such as mass soft-landing techniques and atomic layer loading is not favorable for practical applications. Wet chemical synthesis methods (including hydrothermal, co-precipitation, impregnation, deposition–precipitation, and sol–gel methods), high-temperature pyrolysis, and other methods that can be easily utilized in practice are commonly used. Wet chemistry and high-temperature pyrolysis are gentler, the Fe monatomic precursors are more equally disseminated over the carrier, and the pyrolysis process's high temperature causes the Fe atoms to interact with the heteroatoms to form a stable structure [66]. In addition, factors such as the choice of carriers during the preparation process can affect the efficiency of the iron monoatomic catalysts. Yao et al. prepared a porous carbon (PC) (Fe@COF) that confines single-atom Fe in a covalent organic framework (COF) and tested the effectiveness of Fe@COF for the degradation of organic pollutants when it is used as a catalyst. Iron doping preferentially generated effective single-atom Fe–Nx active sites in the carbon skeleton with electronic structure modulation, conferring outstanding catalytic properties [67].

Metal single atoms, when successfully introduced, can act as polarization centers, thus inducing polarization loss for electromagnetic wave absorption. Furthermore, interactions between metal single atoms and nearby N/C atoms generate charge redistribution, which disrupts the symmetry of the local microstructure and leads to the production of extra electric dipoles, improving electromagnetic wave absorption performance. This also efficiently enhances the heating rate and strength of the electric field surrounding the metal's single atoms, hence improving the effectiveness of single-atom catalysis. In addition, by the coordination of surrounding ligands, single metal centers such as Fe are projected to endure high temperatures after absorbing electromagnetic waves, resulting in high catalytic activity [68–73]. Zhou et al. prepared Fe single atoms anchored on 3D N-doped nanocarbon (3D Fe–NC) using the NaCl template method, and used them under MW irradiation for the removal of chloramphenicol (CAP) contamination from soil. Experiments showed that 3D Fe–NC could enhance electromagnetic wave absorption and had good catalytic performance, and the removal of CAP could reach 99.9% in 5 min [74].

3.4 Other iron-based catalysts

To alter the electromagnetic characteristics of iron-based catalysts, some research has mixed iron-based catalysts with other materials (such as metal powders or conductive polymer composites), and such composite iron-based catalysts are usually synthesized in more than one step, requiring a combination of several preparation methods, such as impregnation and hydrothermal methods. Ai et al. synthesized a FeSx/talc composite material. When exposed to MW radiation, the system quickly liberated its hydroxyl group and sulfate. This resulted in the elimination of a specific concentration of 2,4,6-trichlorophenol in under 4 min, with a maximum COD removal of over 90.1%. Similar novel composites have potential in MW catalysis with their low cost, great physicochemical stability, and high reusability [75]. It is also possible to combine

iron-based materials with common MW absorbers (e.g., carbon-based materials) to improve the MW absorption performance and enhance the catalytic effect. Carbon nanotubes (CNTs) are used as promising MW-absorbing materials to support the nucleation and growth of metal nanoparticles, but carbon nanomaterials alone exhibit slower kinetics and poorer selectivity, and can therefore be combined with poorly dispersed materials with narrower adsorption bandwidths. Liu et al. explored the degradation of methyl orange (MO) in aqueous solution by CNTs loaded with $CuFe_2O_4$ at different additions (1:2, 1:4, 1:8) under MW radiation. Under MW irradiation, the surface of the composites formed h^+, $^{\cdot}OH$, $O_2^{\cdot-}$, and all the active substances together degraded 83% of MO in 5 min, with a TOC removal rate of 91%. The removal effectiveness rose as the quantity of CNTs increased [76].

4 Characterization of iron-based catalysts

The characterization of iron-based catalysts can qualitatively and quantitatively describe the composition-structure-function relationship of the catalysts, which is of significant importance in comprehending the role of their properties and catalytic activity [90]. Most Fe-based catalysts are solid and can be evaluated with suitable characterization methods. This section briefly describes some of the common characterization methods for iron-based catalysts.

4.1 Morphological and microstructural analysis

The size, shape, and distribution of iron-based catalysts can be understood by analyzing the morphology and microstructure. Scanning electron microscopy (SEM) can not only observe the material's three-dimensional structure, but also measure its size, dispersion state, and curvature in some situations, and clear images can be obtained for the surface of complex and rough samples. Transmission electron microscopy (TEM) has a greater resolution than SEM and can get more information about the material's internal microstructure, including a more detailed investigation of the core–shell structure and nanoparticles deposited on the carrier's inner and outer surfaces [91]. To further resolve the atomic-level structure, high-resolution TEM (HRTEM) can accurately measure lattice fringes (e.g., facet spacing, crystal orientation, and length distributions), observe the structure of phase interfaces, and detect the degree of orderliness of atomic arrangement or defects (e.g., dislocations, vacancies) on the surface of the crystals [92]. In MW catalysis, the porous structure or nanoscale particles of the catalyst can increase the exposure of active sites. Zhang et al. used the prepared Co-, Ni-, and Cu-doped iron-based catalysts for MW-assisted catalytic cracking of polyethylene, which showed good catalytic performance. The excellent performance may stem from the special morphology of the catalysts: SEM was employed to characterize the morphology of the catalysts (Figure 3a and b), and it was found that the prepared catalysts showed a sponge-like morphology with many cavities, which was conducive to MW absorption. Furthermore, TEM was employed to characterize the carbon products (Figure 3c and d), and it was found that the obtained solid products consisted of CNTs with inner and outer diameters ranging from 18 to 24 nm, which was consistent with the SEM results [98].

4.2 Crystal structure and phase composition analysis

X-ray powder diffraction (XRD) is commonly used to characterize the phase composition, grain size, lattice parameter, and crystallinity information in solid MW-iron-based catalysts, which affect the catalytic activity and selectivity. In addition, XRD analysis of recycled catalysts and comparison with fresh catalysts can yield data on the changes in the microstructure and crystalline phase of the catalyst, which can be used to speculate on the stability and reusability of catalysts in MW-iron-based systems [96]. Elías et al. conducted research to characterize the crystalline phases of Fe-modified mesoporous nanostructures. They hypothesized that specific iron oxide phases would exhibit better catalytic performance in the microwave-assisted selective oxidation of sulfides. By determining the crystalline phase compositions using XRD (Figure 3e), they provided a basis for understanding the source of the catalysts' activity. This study also indirectly proved the stability of the catalysts by comparing the XRD patterns of the iron-based catalysts before and after MW irradiation and observing the changes in crystalline phase and structure [94].

4.3 Specific surface area and pore size distribution analysis

Specific surface area and pore size are important parameters affecting the storage capacity of materials. For

iron-based catalysts, their specific surface area and pore structure influence MW absorption efficiency via reflection, refraction, or transmission of MWs, which in turn directly affects the availability of reaction sites [97]. Parameters such as catalyst surface area and porosity are usually analyzed on a specific surface area analyzer and calculated using the Brunauer–Emmett–Teller (BET) method. In general, iron-based catalysts featuring high specific surface area and small pore size are conducive to MW absorption, thereby accelerating pollutant degradation or removal. Lounnas and his team newly developed a non-homogeneous iron-based catalyst for the photo-Fenton degradation of methylene blue under MW irradiation, and analyzed the nitrogen adsorption-desorption isotherms using the BET technique to evaluate the specific surface area and pore structure of the iron-based catalyst. Figure 3f shows a type IV adsorption isotherm, proving the mesoporous nature of the catalyst. Meanwhile, the total pore volume was quantified as 0.215 $cm^3 \cdot g^{-1}$, the specific surface area was 23.696 $m^2 \cdot g^{-1}$, and the average pore size was calculated to be 5.409 nm, which confirmed the prevalence of mesopores and facilitated MW absorption. The catalyst achieved 95.5% MB color removal within 8 min of MW irradiation [95].

4.4 Functional group analysis

Functional groups on iron-based catalysts were identified using Fourier transform infrared spectroscopy (FTIR), and the chemical structures were characterized to investigate the correlation between surface properties and performance of iron-based catalysts [98]. Tantuvoy et al. explored the effect of MW-assisted technique for the removal of malachite green (MG) in the presence of spinel-type $CoFe_2O_4$ catalysts. The FTIR spectra of $CoFe_2O_4$ exhibited a characteristic vibrational peak of Fe-O octahedral coordination bonds at 596 cm^{-1} (Figure 4a), indicating the presence of highly active octahedral Fe^{3+} sites in the catalyst. These sites can accelerate electron transfer via the MW-induced thermal effect, thereby promoting the generation of superoxide anions (O_2^-) and hydroxyl radicals ($^{\cdot}OH$). Meanwhile, the vibrational peak of surface hydroxyl groups (−OH) at 3,386 cm^{-1} suggested the adsorption of water molecules on the catalyst surface, which facilitates the decomposition and generation of −OH through MW polarization to participate in MG degradation. Additionally, the density of surface hydroxyl groups detected by FTIR was positively correlated with the $^{\cdot}OH$ generation observed in free radical trapping experiments, further

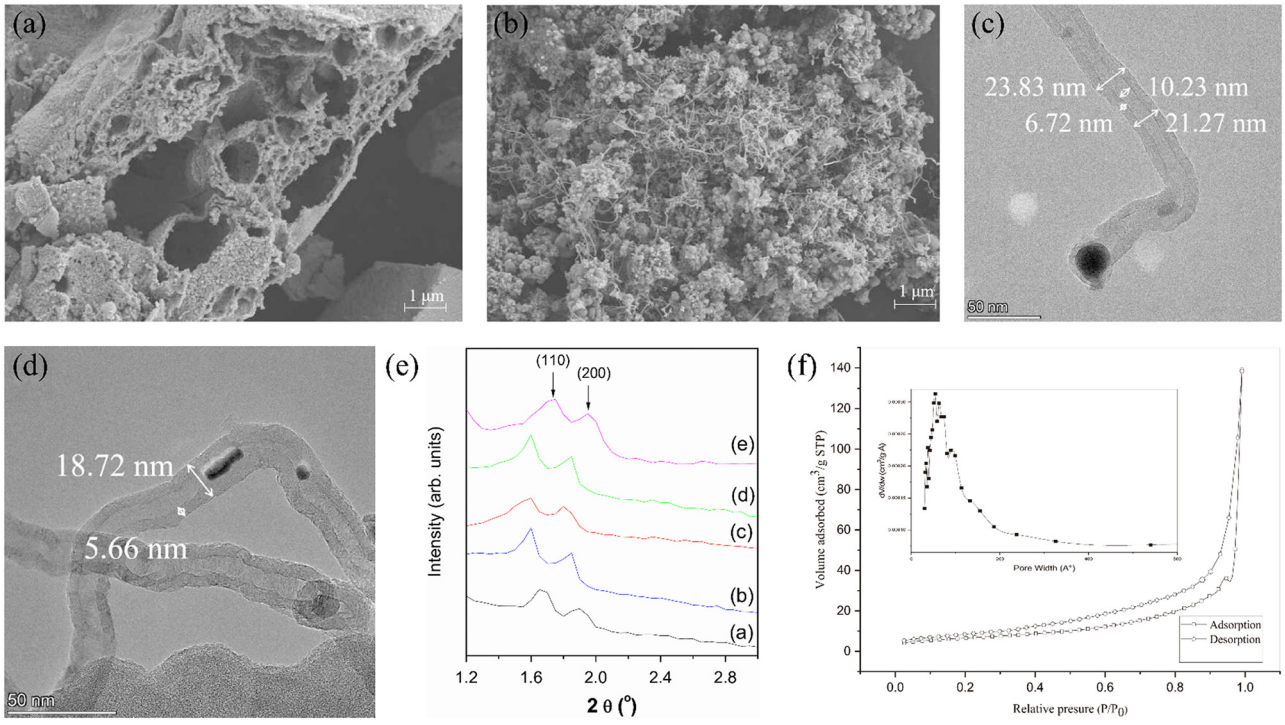

Figure 3: (a and b) SEM images of the catalyst before and after use and (c and d) TEM images of the catalyst. Reproduced from Zhang et al. [93] with permission from Wiley-VCH Verlag. (e) XRD pattern of the synthesized material. Reproduced from Elías et al. [94] with permission from Elsevier. (f) N_2 adsorption–desorption isotherms and pore size distribution curves of Fe–CY catalyst. Reproduced from Lounnas et al. [95] with permission from Elsevier.

confirming that hydroxyl groups serve as key surface moieties for MW-induced free radical production [99].

4.5 Surface elemental composition and valence analysis

The electronic, elemental, and chemical properties of the catalyst surface can be probed using X-ray photoelectron spectroscopy (XPS) [100]. Yuan et al. prepared molecular sieve-loaded oxygen-rich vacancy Fe_2O_3-MnO_2 catalysts (Ov-Fe-Mn@MOS) and proposed a new MW-catalyzed oxidative denitrification method, which was able to deeply oxidize NO to nitrates/nitrites with very small NO_2 generation. In this study, XPS analysis was performed to determine the elemental valence states in the prepared complexes. In Figure 4b, four pairs of Fe $2p_{1/2}$ and Fe $2p_{3/2}$ peaks appear, of which the Fe $2p_{1/2}$ peak at 724.9 eV and the Fe $2p_{3/2}$ peak at 711.3 eV are attributed to Fe(II), the Fe $2p_{1/2}$ peak at 728.3 eV and the Fe $2p_{3/2}$ peak at 713.9 eV are attributed to Fe(III), and the peaks at 719.5 and 734.2 eV are satellite peaks. Combined with the splitting characteristics of Fe $2p_{1/2}$ and Fe $2p_{3/2}$ peaks, the results indicate the presence of Fe(II)/Fe(III) redox pairs in the iron-based catalysts, which facilitate electron transfer under MW irradiation. Meanwhile, the O 1s XPS spectrum revealed lattice oxygen (O^{2-}), surface adsorbed oxygen (O^-/O_2^{2-}), and oxygen vacancies (Ov) on the catalyst surface. Through peak-fitting analysis, the authors quantified the relative content of Ov, which was found to correlate positively with NO oxidizing activity in subsequent experiments. Additionally,

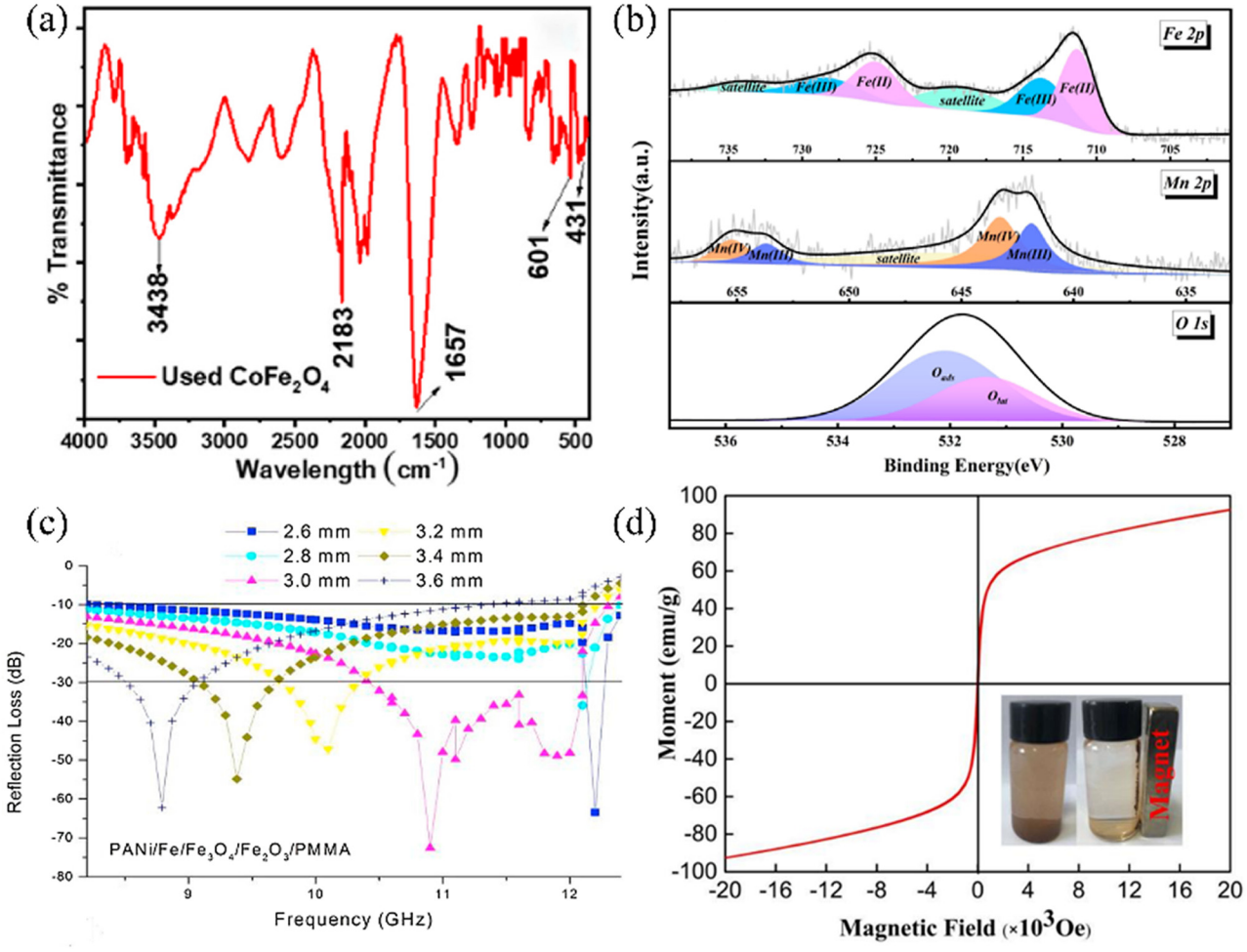

Figure 4: (a) FTIR spectra of synthesized $CoFe_2O_4$ nanoparticles. Reproduced from Tantuvoy et al. [99] with permission from Elsevier. (b) Fe 2p, Mn 2p, and O 1s XPS spectra of fresh Ov-Fe-Mn@MOS. Reproduced from Yuan et al. [43] with permission from ACS. (c) RL for PANi/Fe/Fe_3O_4/Fe_2O_3/PMMA. Reproduced from Peymanfar et al. [105] with permission from Elsevier BV. (d) *M-H* hysteresis loop of C-$ZnFe_2O_4$ composite and (the inset) magnetic separation test for the catalysts. Reproduced from Gao et al. [106] with permission from Elsevier.

Mn doping significantly increased the relative content of Fe^{2+}, presumably due to Mn^{4+}-mediated reduction of Fe^{3+} to Fe^{2+} via electron transfer ($Mn^{4+} + Fe^{2+} \rightarrow Mn^{3+} + Fe^{3+}$), thereby maintaining the Fe^{2+}/Fe^{3+} cycle and enhancing system activity [43].

4.6 Analysis of wave-absorbing properties

The wave-absorbing properties of iron-based catalysts are primarily governed by their electromagnetic parameters, predominantly including the complex dielectric constant and complex permeability. Various influencing factors of wave absorption performance – such as sample reflectivity, dielectric loss, magnetic loss, and impedance matching – are calculated based on these electromagnetic parameters. A vector network analyzer can be employed to test the absorption properties of iron-based catalysts [101]. The wave-absorbing properties of the materials are analyzed using the relative complex permittivity (ε_r) and relative complex permeability (μ_r) calculated by Eqs. 3 and 4. The real part (ε' and μ') and the imaginary part (ε'' and μ'') represent the ability of the wave-absorbing material to store electromagnetic energy and to consume electromagnetic energy, respectively. Two important parameters, the tangent of dielectric loss ($\tan\delta_\varepsilon$) and the tangent of magnetic loss ($\tan\delta_\mu$), calculated by Eqs. 5 and 6, can be used to measure the reflection loss (RL) of wave-absorbing materials [102,103]. The RL at different thicknesses is proposed and calculated according to the transmission line theoretical equations as follows (7) and (8):

$$\varepsilon_r = \varepsilon' - j\varepsilon'' \tag{3}$$

$$\mu_r = \mu' - j\mu'' \tag{4}$$

$$\tan\delta_\varepsilon = \mu''/\mu' \tag{5}$$

$$\tan\delta_\mu = \varepsilon''/\varepsilon' \tag{6}$$

$$Z_{\text{in}} = (\mu_r/\varepsilon_r)^{1/2} \tanh\left[j(2\pi fd/C)(\mu_r\varepsilon_r)^{1/2}\right] \tag{7}$$

$$\text{RL(dB)} = 20 \log \left|\frac{Z_{\text{in}} - 1}{Z_{\text{in}} + 1}\right| \tag{8}$$

where ε', ε'', μ', and μ'' represent the real and imaginary parts of the permittivity and permeability, respectively, ε_r is the complex permittivity, μ_r is the relative complex permeability, $\tan\delta_\varepsilon$ is the tangent to the material's dielectric loss, $\tan\delta_\mu$ is the tangent to the magnetic loss, Z_{in} is the surface normalized input impedance of the absorber, f is the frequency, j is the imaginary part of the complex number, d is the thickness of the absorber, and C is the velocity of light in free space.

The high complex dielectric constant and complex permeability during the MW chemical reaction promote the target pollutants' quick reaction and degradation during the degradation process [104]. In addition, the lower the RL value, the better the MW absorption performance, which may be used in conjunction with Eq. 8 to investigate the materials' MW absorption performance and create iron-based catalysts with good wave-absorbing ability. Peymanfar et al. designed polyaniline (PANi)/Fe/Fe_3O_4/Fe_2O_3 nanocomposites using a complementary radical polymerization and reduction method, as shown in Figure 4c. The PANi/Fe/Fe_3O_4/Fe_2O_3/PMMA nanocomposites exhibited a maximum RL of 72.61 dB at 10.9 GHz and an absorption bandwidth exceeding 1.71 GHz with values over 30 dB at a thickness of 3 mm, demonstrating excellent MW absorption capability [105]. When screening materials for use as MW iron-based catalysts, priority should be given to iron-based materials with superior wave-absorbing properties, as these properties directly influence MW energy conversion efficiency, which in turn affects pollutant treatment efficacy [73,74].

4.7 Magnetic analysis

The magnetic properties of iron-based catalysts are crucial for MW-assisted contaminant treatment, as they are associated with the ease of catalyst recovery from the system. Iron-based catalysts that enable efficient recovery are both economical and environmentally benign. The recovery performance of such catalysts can be evaluated by measuring magnetic parameters – including magnetization intensity and hysteresis loops – using a vibrating sample magnetometer (VSM). Gao et al. prepared C-$ZnFe_2O_4$ (C-ZFO) magnetic composites using a hydrothermal method and used them for the degradation of norfloxacin (NOR) in water under MW irradiation. Typical hysteresis loops of the C-ZFO were measured using the VSM, as shown in Figure 4d. The results of the hysteresis loop show that the saturation magnetization strength of C-ZFO is 92.5 $\text{emu}\cdot\text{g}^{-1}$, which has excellent magnetic properties for magnetic separation and excellent magnetic properties for easy recycling and utilization as compared with the previous studies [106]. In general, saturation magnetization strength is an important parameter of magnetic materials, which determines the maximum magnetization strength and performance of magnetic materials. Magnetic data cannot be considered in isolation when selecting magnetic materials, but need to be further analyzed in conjunction with other characterization methods, and the appropriate

value of magnetization strength needs to be considered in conjunction with the needs of the specific application in order to achieve optimal performance and cost-effectiveness.

5 Application of Fe-based catalysts for the treatment of environmental pollutants under MW irradiation

The introduction of MW irradiation of iron-based catalysts, together with the reactor under different conditions, will produce different effects on the treatment of organic pollutants, heavy metals, pathogenic microorganisms, medical waste, and other contaminants.

5.1 Reaction devices

The heating unit generally consists of three elements: the MW oscillator, the chamber, and the reactor. Where the oscillator is a magnetron or solid-state device, the magnetron cannot adjust the frequency and its output power is the sum of the power at a fixed frequency. The MW oscillator in the early common household MW furnaces was the magnetron, but the lack of temperature and pressure control in the household MW furnaces was not conducive to the repetition of the chemical reaction [107,108]. The heating performance of MW is susceptible to the shape and size of the reactor and the nature of the material [109]. Therefore, the design and development of suitable MW experimental setups contribute to the efficient treatment of pollutants. Depending on the specific reaction needs, MW reactors can be categorized into continuous MW reactors (Figure 5a) and intermittent MW reactors (Figure 5b) [110]. In a continuous MW reactor, MW energy

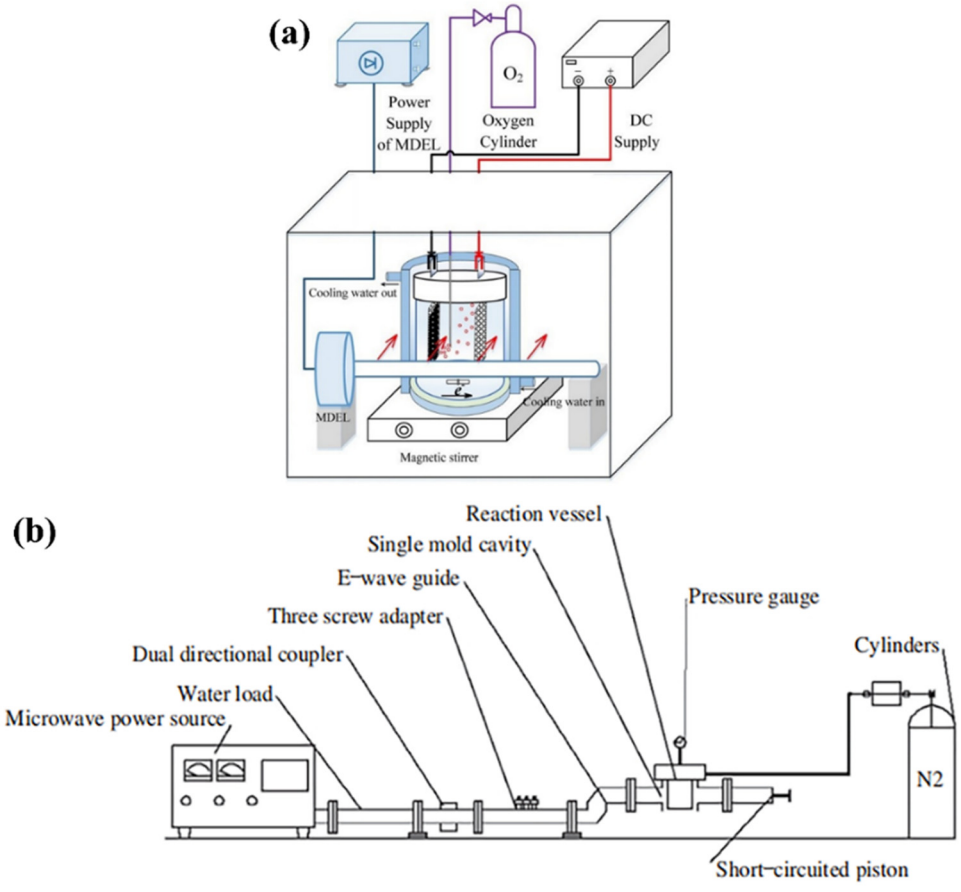

Figure 5: (a) Diagram of a continuous MW reactor. Reproduced from Wang et al. [114] with permission from Elsevier. (b) Schematic diagram of a batch MW reactor. Reproduced from Xue et al. [112] with permission from IOS Press.

is continuously introduced into the reaction system while the reaction material flows through the MW radiation zone in a continuous manner [111]. These reactors typically feature specially designed waveguide structures or MW cavities to ensure uniform distribution of the MW field along the material flow path, enabling the material to absorb MW energy uniformly. They are characterized by large processing capacity, high recovery rate, and no secondary pollution [112]. For an intermittent reactor, materials are added to the reactor in a single batch prior to the reaction, followed by activating the MW to heat the system. During the reaction, MW power can be adjusted according to a preset program, and different intermittent MW reactors vary in their control modes of energy input [113]. Most batch-type MW reactors are adapted from traditional MW furnaces with specialized structures, including temperature control via a water circulation system and an external condensing unit for recovering evaporated liquids.

In a typical MW catalytic treatment of pollutants experiment, a certain amount of catalyst and pollutants were added to containers, which were then sealed and heated in an MW reactor at a set power. While the temperature of the reaction was controlled, the reaction was finished with the use of the appropriate quencher agent to quench the mixture, after which the reactants and catalyst were separated and further analyzed [115,116]. At the end of the experiment, the removal rate was calculated.

However, the application of MW technology in iron-based catalysis, especially for large-scale upscaling, presents numerous challenges in reactor design and operation: (1) heat dissipation and safety concerns. Safety issues during MW reactions primarily involve explosion risks and container damage. MW heating of volatile reactants or reactions under high-pressure conditions may lead to uncontrolled reactions and explosions. Additionally, polar acid-based reactions (e.g., systems containing concentrated sulfuric acid) can cause rapid temperature increases, melting containers, and posing hazards. MW leakage can damage body tissues and cells – studies have shown that MW radiation induces distinct DNA strand damage compared to conventional heating under the same thermal conditions, causing habitual DNA strand damage [117]. (2) Electromagnetic field distribution and energy transfer issues. In traditional fixed-bed reactors, MW fields are unevenly distributed, with sharp particle contacts prone to triggering localized overheating (hot spots). This issue becomes more pronounced with increased catalyst filling volume (as noted in Chen et al.'s research). Furthermore, MW-absorbing coke formed during reactions exacerbates arc discharge, further interfering with reaction control [118]. (3) Skillful design of MW energy ports. As reported by Yan et al., improperly positioned MW energy input/output ports can significantly reduce energy efficiency. In large-scale reactors, MW transmission characteristics are more complex (e.g., rectangular traveling-wave MW reactors exhibit a mix of standing and traveling wave behaviors, hindering uniform energy distribution and efficient transmission) [119].

The quantification of energy efficiency is a critical component in evaluating reaction performance. In MW-iron-based systems, diverse factors – such as reactant properties, iron-based catalyst characteristics, and reactor structure – have led to inconsistent energy efficiency quantification methods across studies, with no unified and widely accepted standard yet established. For example, some research uses the ratio of energy consumed for chemical bond breaking and product formation to the total MW energy input during the target reaction as an efficiency metric [119]. Others adopt energy consumption per mole ($kJ \cdot mol^{-1}$) as an indicator, defining it as the energy (in kilojoules) required to produce each mole of product. This metric decouples productivity from the time factor, enabling purer comparisons of energy consumption performance across different reactors. Notably, this indicator has been used to conclude that MW reactors are more energy-efficient than pilot-scale conventional reactors in laboratory-scale comparisons [120]. In addition, a study has quantified the energy efficiency of the MW heating process and explored the factors affecting the efficiency, providing a direction for optimizing the MW heating process. The MW heating process is divided into two stages, the conversion from input electrical energy to MW energy, and the conversion from MW energy to effective heat energy, and the energy conversion efficiencies of the two stages are defined: the first stage efficiency $\eta_1 = Q_{MW}/Q_{net}$, the second stage efficiency $\eta_2 = Q_{eff\text{-}heat}/Q_{MW}$, and the total efficiency $\eta = \eta_1 \times \eta_2$. Measuring the input electrical energy Q_{net}, the MW energy Q_{MW} is obtained by monitoring the anode voltage and current, and then the effective thermal energy $Q_{eff\text{-}heat}$ is calculated by considering the heat absorption and heat loss of the medium and vessel. Meanwhile, it is also proposed that the energy efficiency can be optimized by changing the position of the heating body, selecting the appropriate heating medium, reasonably designing the medium volume, and increasing the MW output power [121].

5.2 Treatment objects

Sorting out the substances handled by iron-based MW catalysts will help to carry out targeted research and maximize the benefits of the catalytic system. This section

Table 2: List of some typical contaminants removed using iron-based catalysts combined with MW irradiation

Catalyst	Contaminant	Reaction condition	Degradation efficiency % (min)	Stability and reusability	Strengths, weaknesses, and suitability	Refs.
GAC/ZVI	Carbofuran	[CB] = 100 mg·L^{-1}; volume = 250 mL; catalyst dose = 0.2 g·L^{-1}; output power = 750 W.	79% (0.5)	—	Deep mineralization can be achieved with complex pH effects. Suitable for the removal of highly concentrated pollutants, such as pesticide production wastewater	[140]
Fe^0	Chlorobenzene (CB)	[CB] = 100 mg·L^{-1}; volume = 40 mL; catalyst weight = 1 g; output power = 250 W	82.8% (5)	—	The reaction conditions are mild and the reaction mechanism is complex and difficult to control precisely. It can be used in the treatment of chlorobenzene-containing wastewater generated in industrial production, and the treatment of chlorobenzene-contaminated soil leachate and other scenarios	[62]
$CaFe_2O_4$/PNA	MTZ	[MTZ] = 90 mg·L^{-1}; volume = 100 mL; catalyst weight = 100 mg	94% (21)	After 5 cycles of use, there was no significant loss of catalytic activity, and the degradation rate was 86%	Environmentally friendly, material preparation is more complicated and may face process complexity and cost problems when scaling up production. Suitable for the pretreatment of high-concentration antibiotic wastewater	[126]
Co–$Bi_{25}FeO_{40}$	BPA	[BPA] = 60 mg·L^{-1}; volume = 100 mL; catalyst dose = 1.2 g·L^{-1}; output power = 250 W; pH = 9; temperature = 60°C	92% (5)	XRD, FTIR, and SEM-EDAX showed structural integrity and 80.6% degradation after five applications	Highly resistant to interference, adaptable to complex water quality, and synchronized with disinfection capability. Non-free radical mechanism has limitations. Suitable for BPA-containing wastewater treatment that requires simultaneous degradation and disinfection	[136]
xFe_2O_3/ $LaCu_{0.5}Co_{0.5}O_3$-$MMT_{0.2}$	BPA	[BPA] = 50 mg·L^{-1}; volume = 50 mL; catalyst dose = 9.5 g·L^{-1}; output power = 500 W; pH = 4	97.7% (6)	The leaching rate of Fe after 5 cycles was 0.019% and the degradation rate was 95.4%	Process parameters are adapted to a certain range of parameter fluctuations. Complex preparation process. Suitable for the rapid degradation of highly concentrated BPA wastewater	[141]
Spinel zinc ferrite (SZFO)	Brilliant green (BG)	[BG] = 20 mg·L^{-1}; volume = 50 mL; catalyst weight = 0.05 g; output power = 360 W; pH = 11	99% (5)	—	Wide process adaptability, high concentration intermediate products may have short-term toxicity. It is suitable for the treatment of organic dye wastewater in low and medium concentrations	[142]
Fe_3O_4	PNP	[PNP] = 20 mg·L^{-1}; volume = 100 mL; catalyst dose = 0.1 g·L^{-1}; pH = 3; temperature = 80°C	98.2% (28)	After 3 cycles of recycling, there was no significant change in Fe_3O_4 morphology and the degradation rate was 93.4%	Low energy consumption and wide environmental adaptability. Long-term use may accumulate heavy metal ions. Suitable for the treatment of organic wastewater containing PNP in low and medium concentrations	[143]

(*Continued*)

Table 2: *Continued*

Catalyst	Contaminant	Reaction condition	Degradation efficiency % (min)	Stability and reusability	Strengths, weaknesses, and suitability	Refs.
Fe_3O_4	Pyrene	[Pyrene] = 50 mg kg^{-1}; catalyst dose = 40 mg; temperature = 60°C	91.7% (45)	After four times of reuse, there is about an 80% degradation rate	Suitable for soils with low to medium concentrations of pyrene pollution, adaptable to complex soil substrates, and low toxicity. Follow-up treatment (e.g., lime addition) is required to control ionic residues	[144]

describes the treatment objectives for each aspect of MW catalysis (Table 2).

5.2.1 Organic pollutants

Organic pollutants are by far the most widely utilized type of pollutants treated by iron-based MW catalysts. In general, when organic molecules on the catalyst surface are irradiated by MW, high temperatures are generated at the hot spots, which excite the system to generate h^+, $^{\cdot}OH$, $O_2^{\cdot-}$, and other active substances to attack the organic pollutant molecules and degrade the pollutants [122], as shown in Eqs. 3–10:

$$MW + catalyst \rightarrow h^+ + e^- \quad (9)$$

$$H^+ + H_2O \rightarrow HO^{\cdot} + H^+ \quad (10)$$

$$h^+ + OH^- \rightarrow HO^{\cdot} \quad (11)$$

$$e^- + H_2O_2 \rightarrow HO^{\cdot} + OH^- \quad (12)$$

$$e^- + O_2 \rightarrow O_2^{\cdot-} + H^+ \quad (13)$$

$$O_2^{\cdot-} + H_2O_2 \rightarrow {}^1O_2 + OH^- + HO^{\cdot} \quad (14)$$

$$O_2^{\cdot-} + HO^{\cdot} \rightarrow {}^1O_2 + OH^- \quad (15)$$

$$HO^{\cdot} + contaminants \rightarrow H_2O + CO_2 \quad (16)$$

5.2.1.1 Pharmaceuticals and personal care products (PPCPs)

PPCPs are emerging contaminants I, including a wide range of substances such as antibiotics, analgesics and non-steroidal anti-inflammatory drugs, antiepileptic drugs, β-blockers, antineoplastic agents, disinfectants, synthetic musks, some preservatives, and some sunscreens, and the conventional treatment processes are often ineffective in removing these compounds, which can pose a significant risk to human health and other organisms posing significant risks [123,124]. In the face of such difficult to treat pollutants, MW irradiation combined with iron-based catalyst system shows good prospects for application. It has been shown that this system is capable of efficiently degrading a wide range of PPCPs. For example, in the experiments of Vieira et al., excellent combined degradation was observed when ibuprofen, ketoprofen, and diclofenac were treated under MW irradiation using activated carbon loaded with $CuFeS_2$ nanoparticles (ACFS) as a catalyst: all three target pollutants achieved complete mineralization within 20–30 min, the degradation process conformed to the pseudo-primary kinetic model, and the catalyst maintained good activity after 10 consecutive

cycles [125]. This efficient degradation process is attributed to a key mechanism triggered by the synergistic interaction of MWs with iron-based catalysts, i.e., MWs promote efficient electron-charge transfer at the catalyst surface and induce the formation of "hot spots," which significantly enhances the generation of strongly oxidizing hydroxyl radicals. Similarly, the study of Zia et al. synthesized PNA/$CaFe_2O_4$ nanohybrids using MW-assisted technique. They found that metronidazole (MTZ-90) at a concentration of 90 mg·L^{-1} could be degraded up to about 94% within 21 min of MW irradiation when the PNA loading was 40%. As a comparison, the degradation rate of MTZ-90 by MW irradiation alone without a catalyst was only 41%. The free radical scavenging experiments further verified that the active species, such as $^{\cdot}H$, $^{\cdot}OH$, and $O_2^{\cdot-}$, produced in the system played a key role in attacking the drug molecules and achieving efficient degradation [126].

5.2.1.2 Phenolic substances

Phenols are one of the main priority pollutants, non-biodegradable and stubbornly accumulative, acting at very low concentrations and existing in a wide range, which are prone to adversely affect the environment and organisms' health [127,128]. Ren et al. investigated a new MW-Fe/Cu system and selected *p*-nitrophenol (PNP) as a model pollutant to evaluate the treatment efficiency of the system. Different doses of Fe/Cu bimetallic particles were added to 100 mL of PNP solution with different initial concentrations, while different initial pH and initial MW power were adjusted, and control experiments were performed. The results showed that the MW-Fe/Cu system could remove 95% of PNP in 2.25 min, and the removal efficiency was much higher than that of the other systems, and it could be used to treat wastewaters containing ultra-high concentrations of toxic and difficult-to-degrade pollutants in a very short period [42].

5.2.1.3 Azo dyes

Dyes are widely used in many industries, such as paper, textiles, food, leather, and printing. In particular, azo dyes account for about 70% of the annual production and 60% of the total use of dyes globally and are highly carcinogenic and mutagenic [129–131]. There is a need to explore economically and operationally simple methods of dye treatment [132]. It has been found that MW radiation enhances the active sites on the catalyst surface, which in turn improves the catalytic performance and has practical applicability for dye wastewater. Mao et al. used nZVI to remove MG under MW irradiation and found that MG was effectively degraded within a short hydraulic residence time [133]. Liu et al. prepared a $CuFe_2O_4$/CNT catalyst with strong MW absorption capacity, and found that the system removed 83% of MO within 5 min, which has potential in the treatment of azo dye wastewater [76].

5.2.2 Heavy metals

Heavy metals have highly toxic elements that are persistent and can have a magnifying effect throughout the food chain [134]. The iron-based catalyst undergoes both "thermal" and "non-thermal" effects under MW irradiation, accelerating the treatment rate of heavy metal contaminants. Li et al. developed a zero-valent iron/pyrite (FeS_2/ZVI) catalyst and combined it with MW irradiation for the treatment of strongly alkaline high Cr(VI) contaminated (SAHCR) soil. This method resulted in 99.9% removal of Cr(VI) within 10 min; the activation energy was reduced by 28.5% with MW irradiation than without MW irradiation. The remediated soil has good long-term stability and provides a reference for treating SAHCR soil with iron-based catalysts under MW irradiation [135].

5.2.3 Pathogenic microorganisms

Pathogenic microorganisms are a type of microorganism that can invade human or animal bodies, causing infections and even infectious diseases. Under certain conditions, the combined system of MW and iron-based catalysts can inactivate bacteria. Li et al. investigated the co-activation of disulfates (PDS) by cobalt-doped $Bi_{25}FeO_{40}$ catalyst and MW, which can play a role in the purification and disinfection of organic pollutants. The energy transfer and cross-coupling reaction induced by MW contributed to the generation of abundant reaction sites on the Co-$Bi_{25}FeO_{40}$/MW/PDS composite. MW energy, catalyst and oxidant could act on *Escherichia coli* at the same time, forming physical pressure and oxidative pressure to make the cell damage, the reaction of 1 min after the cell density decreased dramatically, 5 min after the bacterial death [136].

5.2.4 Medical waste

The status of medical waste is an important public health issue worldwide, and the COVID-19 pandemic has increased global awareness of medical waste disposal over the past few years [137]. Traditional methods of treating medical waste are not enough to fully meet the

needs of medical waste treatment [138]. Yuwen et al. investigated the mechanism of MW-assisted iron-based catalyst pyrolysis of waste COVID-19 masks. The plastic itself was weakly responsive to MW, and the addition of a catalyst not only promoted the deconstruction of the plastic but also increased the uptake of MW. The enrichment state of Fe in the hydrogen-reduced $FeAlO_x$ catalysts was changed, and Fe_3O_4 and FeO, which were highly absorbent to MW, appeared, with good decomposition ability for polyolefin-based disposable medical masks. It provided a reference for chemical recycling of polyolefin plastics [139].

5.3 Factors affecting the treatment effect of environmental pollutants

MW catalysis is a complex process; the specific reaction mechanism is not clear, and a variety of factors will have an impact on the treatment effect of the sample (Figure 6). A reasonable summary of these parameters can help optimize the subsequent experimental design and improve the catalytic efficiency.

5.3.1 pH

The pH has a significant effect on the catalytic performance of MW-Fe-based catalyst systems, which is mainly achieved by modulating the catalyst surface properties, the generation of reactive oxygen species, and the ionization and dissociation states of the adsorbed molecules [90,145], which in turn determines the pollutant removal efficiency. Several studies have shown that the effect of pH on pollutant degradation efficiency varies in different MW catalytic systems. For example, alkaline conditions are favorable in some systems to promote the loss of electrons from OH^- to generate $^{\cdot}OH$, which enhances the oxidative attack on pollutants and leads to an increase in the removal rate with increasing pH [146]. However, a comprehensive analysis showed that the degradation efficiency was not a single trend in response to pH. Xu et al. successfully prepared a six-linear hydrotrope by the precipitation method for the MW-assisted degradation of MO in artificial dye wastewater. The degradation rate of MO showed a trend of increasing and then decreasing with the change of pH in the initial pH range of 3–11 and reached the highest value under neutral conditions (pH = 7) (97.3%). This phenomenon may be attributed to the interaction between the electrical properties of MO molecules (negatively charged at pH > 3.4) and the catalyst surface charge, especially under alkaline conditions, where enhanced electrostatic repulsion significantly inhibited the adsorption process of MO on the catalyst surface [29].

5.3.2 Inorganic anions

Concentrations of inorganic anions such as NO_2^-, HCO_3^-, HCO^-, NO_3^-, and SO_4^{2-} range from 10^{-5} to 10^{-3} M, depending on geography and human activity [147]. To understand how these environmental elements affect the effect and mechanism of MW catalysis, the researchers reported their different findings. Gogoi et al. synthesized a Cu-CFPC

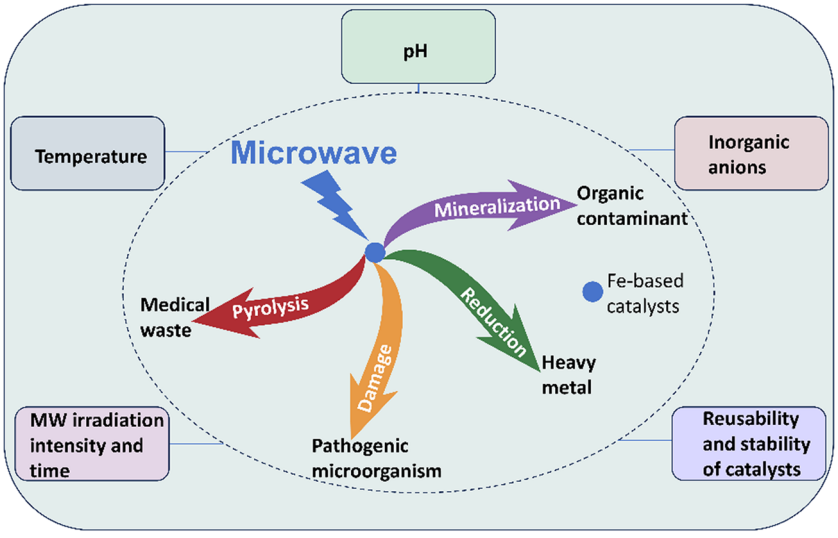

Figure 6: Objects and influencing factors of environmental pollutants treated by Fe-based catalysts under MW irradiation.

catalyst by immobilizing Cu and $CoFe_2O_4$ nanoparticles (CF) on hierarchical PC of coconut fibers. The effect of the presence of inorganic anions on antibiotics was investigated by using this catalyst for the degradation of sulfamethoxazole in the presence of common anions such as Cl^-, NO_3^-, HCO_3^-, and SO_4^{2-} (0.1 M) under MW assistance. According to the results of the study, the degradation rate decreased from the previous complete degradation to 89%, 87%, 81%, and 72% when SO_4^{2-}, NO_3^-, HCO_3^-, and Cl^- were present, respectively. The possible reason for this was that these anions act as scavengers of $^{\cdot}OH$, h^+. These products were less active compared to $^{\cdot}OH$ and therefore degradation rates were reduced [148].

5.3.3 Intensity of MW irradiation

In general, an increase in the intensity of MW irradiation resulted in higher pollutant removal efficiencies, which may be because the steadily increasing power of the MW catalytic system promoted rapid molecular migration. In addition, MW energy produced molecular polarization, which led to electronic vibrations and heat generation [149]. The removal efficiency remained unchanged when the MW irradiation reached a certain intensity, which was since too high an output power cannot sustainably enhance the catalytic activity of the process. Reasonable MW output power not only removes pollutants quickly but also saves energy consumption. Moradi et al. used the sulfonated metal-organic skeleton Fe_3O_4@MIL-100(Fe)-OSO_3H loaded on iron oxide nanoparticles as a catalyst to decolorize aqueous solutions containing MO dyes. The effect of varying the MW power in the range of 100–500 W on the degradation efficiency was investigated, and it was found that the MO degradation rate increased with increasing MW power, which was attributed to the enhancement of "hot spots" on the surface of the catalyst and the formation of hydroxyl radicals in the aqueous solution at higher MW power, resulting in higher degradation efficiency [150].

5.3.4 Temperature

The dielectric properties of catalysts are closely related to temperature. In most cases, as the reaction temperature increases, the contaminant removal enhances accordingly. On the one hand, the high temperature itself is close to the reaction temperature, which tends to accelerate the reaction. On the other hand, at higher temperatures, the "hot spot" effect and selective heating of substances become more pronounced, and the system absorbs MW energy to stimulate molecular rotation and reduce the activation energy of the reaction, which promotes the breaking of chemical bonds and the adsorption of substances. Remya and Lin studied the removal of carbofuran in the MW-assisted granular activated carbon (GAC)/ZVI/H_2O_2 system at different reaction temperatures (30, 50, and 80°C). The degradation rate of carbofuran was accelerated at 80°C, indicating that this temperature was favorable for MW-assisted degradation of the substance [140].

5.3.5 Reusability and stability of catalysts

The stability and reusability of iron-based catalysts is one of the core parameters to consider for their economic utility. However, the reuse process faces physical loss and deactivation due to chemical changes. Physical loss is mainly reflected in the small amount of catalyst loss caused by recycling, washing, drying, etc. For example, Shen et al. found that $NiFe_2O_4$/natural mineral catalysts showed a small decrease in degradation efficiency after reuse, which was mainly attributed to nanoparticle loss during the above-mentioned operations, and the conventional magnetic separation recycling also suffers from the risk of such physical loss [30]. A more serious challenge comes from chemical changes, especially the reduction of activity (passivation) due to Fe leaching. To control such deactivation in the MW-Fe system, three key mechanisms have been revealed: (1) bimetallic synergy, e.g., the introduction of Co to form Fe-Co bimetallic sites, which reduces the overconsumption of a single metal site through a synergistic effect, thereby reducing the risk of leaching; (2) the protective effect of carbon-based carriers, e.g., the anchoring of Fe in the form of a monoatom on a three-dimensional nitrogen-doped carbon-carrier to form a stable Fe–N coordination structure, which effectively inhibits iron agglomeration and leaching; and (3) MW-specific effects, the above structure can simultaneously enhance MW absorption, which helps to maintain the stability of the active sites. In addition, for unavoidable deactivation, an effective regeneration strategy is crucial. Among them, thermal regeneration (calcination) has been proven effective, e.g., He et al. showed that the catalytic performance of the inactivated iron-based catalysts after use could be significantly restored by calcining them at 400°C for 30 min [151]. In contrast, Chang Zhou's study significantly improved the intrinsic stability of the material by the optimized carrier design itself, thus reducing the need for regeneration [74].

Based on the principle of the action of iron-based catalysts under MW irradiation, combined with the above influencing factors reported in previous studies, a

theoretical framework for parameter screening can be initially established. After that, single-factor variable experiments were carried out to examine the degree of influence of each parameter on the reaction one by one. After the initial screening of single-factor experiments, response surface methodology can be used to systematically analyze the effects of multi-parameter interactions on performance. For example, Wang et al. used response surface methodology to establish a mathematical model to optimize the experimental design using the degradation rate of BPA as an indicator to obtain better experimental process parameters. The effects of reaction time, solution pH, MW power, and other factors on the experiment were investigated. Experiments on the degradation of BPA by iron-based catalysts were carried out using the BBD model. A quadratic model equation was used to predict the relationship between the response (BPA removal rate) and the three variables, and the parameter values that could lead to complete degradation of BPA were finally determined [141].

5.4 Toxicological evaluation

When using iron-based catalysts to treat pollutants under MW irradiation, the toxicity evaluation of by-products is an important part of assessing the environmental safety of the technology. Current studies have focused on the toxicity of degradation products of organic pollutants, and the patterns and mechanisms of toxicity changes have been revealed by various analytical methods. Existing studies have shown that MW irradiation combined with an iron-based catalyst system can usually reduce the toxicity of pollutants. For example, Gao et al. evaluated the acute toxicity of NOR degradation products using the *Vibrio fischeri* luminescence inhibition assay (ISO 11348-3-2007 standard) and found that the toxicity of the solution treated with the MW/Iron-based catalyst/PS system was significantly lower than that of the original pollutant, although the toxicity showed irregular fluctuations with reaction time. He et al. used the toxicity evaluation software (ECOSAR) to analyze the toxicity of the degradation products of pantethine glucosamine (DTZ) to fish, daphnia, and algae, and the results showed that most of the intermediates were not significantly or chronically toxic, and only a few intermediates showed a chronic and highly toxic effect on daphnia. These studies suggest that MW-induced iron-based catalytic reactions can promote deep mineralization of pollutants through the "hot spot" effect, thus reducing the accumulation of toxic intermediates [106,151].

However, there are some limitations in the current research. On the one hand, most of the work is focused on a single pollutant, and there is a lack of by-product toxicity assessment of multiple and complex real-world environmental systems (e.g., heavy metal-containing or plastic-containing). On the other hand, the toxicity assessment methods are relatively homogenous, relying mainly on bacterial toxicity tests or software predictions, but lacking more comprehensive assessments of chronic toxicity and genotoxicity in higher organisms (e.g., fish, mammalian cells). Future studies could combine more advanced analytical tools, such as high-resolution mass spectrometry (LC-HRMS), with non-targeted screening techniques to accurately characterize the structure of degradation intermediates and establish their quantitative relationship with toxicity. Meanwhile, it is recommended to use the combination of multi-species bioassay (e.g., algae-fish three-level system) and computational toxicology modeling (e.g., QSAR) to build a more complete toxicity risk assessment system. In addition, for the composite pollutants in real wastewater, the effect of the MW-iron-based catalytic system on the toxicity transformation needs to be further explored to promote the application of this technology in real environmental treatment [152,153].

5.5 Utilization of density functional theory (DFT) in the treatment of environmental pollutants with Fe-based catalysts under MW irradiation

DFT can accurately calculate energy, charge, molecular orbitals, and other parameters, explore the atomic structure of catalysts and directly identify active sites, and use the intrinsic properties of atoms to predict the physical/chemical properties of materials, gradually becoming an irreplaceable aid in experiments [154,155]. He et al. used MW-assisted dielectric activation of a dual-responsive Co/Fe carbon-based catalyst (CoFe/NC-3) to activate peroxynitrite to achieve an efficient degradation of DTZ, with a degradation rate of up to 100% within 6 min. The Fukui exponential isosurface and Fukui function of DTZ were calculated by the density flooding method to verify the degradation pathway of DTZ [151]. Wang et al.'s team prepared an iron-based magnetic nanomaterial and applied it to the MW-catalyzed degradation of NOR, and the degradation pathway of NOR in this system was hypothesized by DFT calculations [156].

For iron-based catalysts, the main parameters to be considered in the calculations include exchange-

correlation functional, basis set, pseudopotential, spin polarization, and dispersion correction [157–161]. At present, in the study of MW-iron-based catalyst systems, some works have been carried out with the help of DFT calculations to analyze the reaction mechanism and predict the catalytic performance, etc., but the exploration of the specific parameters of the DFT used (generalized function, basis group, etc.) has not been involved. Key parameters such as the electronic structure, adsorption energy, and reaction energy barriers of the iron-based catalysts were predicted by DFT calculations, which provided a theoretical basis for the experimental design in terms of the optimization of Fe–O bonding, O_2 activation mechanism, and the enhancement of MW absorption performance, according to Pan et al. For example, the adsorption energy and reaction energy barriers of O_2 for Fe_3C materials with different oxygen doping amounts (FeCO-1, FeCO-2, FeCO-3) were calculated by DFT. The results showed that the O_2 adsorption energy of FeCO-2 was higher than that of Fe_3C and reduced the Gibbs free energy for the conversion of O_2 into superoxide radical (O_2^-), so FeCO-2 was preferred as the catalyst in the subsequent experiments. The subsequent degradation performance experiments verified that FeCO-2 could be generated O_2^- efficiently in the MW field and realized the rapid degradation of pollutants. In addition, DFT calculations revealed that the introduction of Fe–O bonding changes the electronic structure of Fe_3C, reduces the material band gap, and lowers the conduction band potential to −0.58 V (vs NHE), which is lower than the standard potential of O_2/O_2^- (−0.33 V), theoretically allowing photogenerated electrons to reduce O_2 to O_2^-. Combined with the experimental cyclic voltammetry and electrochemical impedance spectroscopy results, FeCO-2 is more electrochemically active and has a lower resistance to electron transfer, confirming the mechanism of electronic structure optimization predicted by DFT [162]. Yuan et al. [163] speculated the possible reactions in the intermediates by DFT calculations, calculated the Gibbs free energies of the reduction of $*Cr_2O_7^{2-}$ to CrO_3H_3 on the catalyst surface, and made a DFT model structure of the reduction kinetics of Cr(VI): the free energy level diagrams (Figure 7), which revealed, from the atomic scale, the relationship between Cr(VI) groups and the $ZnFe_2O_4$ under positive and negative electric fields, and combined with the experimental results, the rational mechanism of MW-catalyzed Cr(VI) reduction was finally revealed [163].

Combining the existing research, the application of density generalization to mechanisms can be enhanced in two ways. First, the microscopic mechanism modeling of the hot spot region is carried out. The active sites on the catalyst surface are analyzed, the typical crystal surface model of iron-based catalysts is constructed, defects such as oxygen vacancies are introduced, and the electronic density of states under the equivalent conditions of MW fields is calculated to analyze the effect of the d-band center shift of iron atoms on the activation of active sites. And the reaction paths and energy barriers are calculated. Second, the temperature-reaction rate constant correlation model is established through variable temperature DFT calculations, which is combined with equivalent electric field simulations to reveal the synergistic mechanism of MW nonthermal and thermal effects [164–166]. DFT has not yet been fully applied to MW iron-based catalyst systems to explain the mechanisms and pathways, so it is still a long-term process to further carry out and improve the theoretical calculations, and ultimately to realize the theory-guided practice.

5.6 Feasibility assessment of MW iron-based catalytic systems

The MW iron-based catalytic system can efficiently degrade a variety of environmental pollutants through the synergistic effect of MWs and iron-based catalysts, and it shows certain

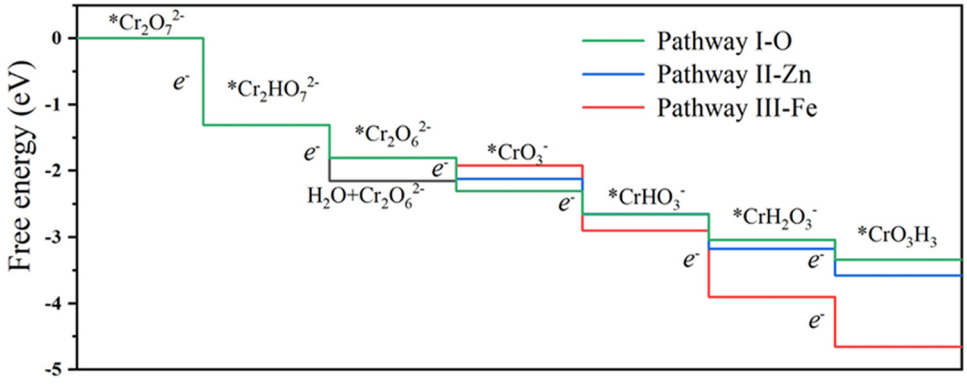

Figure 7: DFT model structure of Cr(VI) reduction kinetics: free energy level diagram. Reproduced from Yuan et al. [163] with permission from Elsevier.

advantages in energy consumption and chemical costs, for example, in the treatment of nitrobenzene wastewater, the MW-assisted iron-based catalyst system can achieve high degradation efficiency in a short period of time, and the power consumption is significantly reduced compared with the traditional heating method, which indicates that the MW iron-based system has certain technical advantages [167]. In addition, rational optimization of MW parameters (e.g., power, radiation time) and catalyst dosage can reduce chemical costs. In the MW iron-based catalyst system for treating environmental pollutants, the cost estimation is mainly carried out in terms of chemical cost and power demand. Taking the removal of pollutants from water as an example, the following equations can be used to determine the power consumption and operating costs [110]:

$$\text{Power consumed (in kWh)} = \frac{\text{MW power} \times \text{time}}{1{,}000 \times 60} \quad (17)$$

$$\text{Pollutant removed/power/catalyst} = \frac{(C_0 - C_e) \times V}{\text{power consumed} \times \text{mg of catalyst}} \quad (18)$$

$$\text{Total operating cost} = E_\chi \text{ cost} + \text{cost of } C_\tau \quad (19)$$

$$E_\chi \text{ cost (\$/kg of } P_r) = \frac{E_\chi(\text{kWh}) \times e_\phi(\$/\text{kW h}) \times 10^6}{(\text{mg of } P_r) \times V(\text{L})} \quad (20)$$

$$C_\tau \text{ cost (\$/kg of } P_r) = \frac{C_\tau \text{ required(kg/L)} \times \text{unit cost of } C_\tau(\$/\text{kg}) \times 10^6}{(\text{mg of } P_r) \times V(\text{L})} \quad (21)$$

where C_0 and C_e represent the initial and final concentrations of pollutants, respectively, P_r represents the amount of pollutants removed, E_χ represents the energy, C_τ represents the cost of chemicals, and V represents the volume of contaminated water samples (in liters).

In practical applications, factors such as catalyst stability and regeneration, complexity of regulating reaction conditions, equipment design and scale-up challenges, initial investment and operating costs, and applicability to actual working conditions may limit the effectiveness of MW iron-based catalyst systems in treating pollutants. The choice of this technology needs to be made in the context of the cost of the system and practical factors.

5.7 Combined techniques for enhanced MW catalysis

As mentioned earlier, MW-iron-based catalyst processes have been coupled with persulfate-based advanced oxidation processes, Fenton/Fenton-like processes for the treatment of specific types of pollutants, and the addition of catalysts can further activate the MW coupling of the above systems [21].

Different technical means complementing each other can achieve better results. photocatalytic technology is considered a mature technology, but the process of water treatment can only deal with high transparency of the low concentration of organic wastewater, for high concentration of organic wastewater or turbid wastewater needs to carry out effective pre-treatment. Whereas MW catalytic technology can treat turbid, colored, highly concentrated organic wastewater without any pretreatment and can shorten the treatment time, the combination of the two technologies may be an effective way to treat different concentrations of organic pollutants in water quickly and thoroughly. Wang et al. constructed a novel Z-type $SrTiO_3$/$MnFe_2O_4$ catalytic system with MW-ultraviolet (MW-UV) dual-responsive activity for the degradation of tetracycline pollutants in water. The results showed that the catalyst exhibited high catalytic activity under the MW-UV system, and the MW plasma generated in the system accelerated the electron transfer and the separation of e^-–h^+ pairs, which promoted the redox capacity and the degradation of the organic pollutants, the $SrTiO_3$/$MnFe_2O_4$/MW-UV showed promising results, with $^{\cdot}OH$ playing a significant role, and the overall indicated that the $SrTiO_3$/$MnFe_2O_4$/MW-UV has good potential in treating different concentrations of antibiotics in wastewater is promising [168].

6 Summary and outlook

This article reviews the research progress of Fe-based catalysts used for MW catalysis to remove relevant pollutants, briefly introduces the preparation methods and characterization techniques of Fe-based catalysts, summarizes the reaction devices and treatment objects of Fe-based catalysts for the treatment of environmental pollutants assisted by MW, and evaluates the effects of pH, inorganic anions, MW irradiation intensity and time, temperature, reusability and stability of catalysts on the pollutant treatment effect. The use of DFT in the treatment of environmental pollutants with iron-based catalysts under MW irradiation is described, as well as the enhanced effects of MV in combination with other technologies. However, the study of iron-based catalysts in MW catalysis is not yet in-depth, and many challenges deserve further work. The following recommendations are made for future work:

(1) Prioritize the development of efficient and economical iron-based catalysts. The type and morphological

structure of catalysts are the key factors affecting their performance. At present, there is still room for improvement of iron-based catalysts in terms of activity and cost. In the future, we should focus on exploring new synthesizing methods and precisely controlling the structure of catalysts to make them have a larger specific surface area and more active sites. At the same time, doping modification of the catalysts is carried out to regulate the electronic structure of the catalysts by introducing transition metal elements (e.g., cobalt, nickel) or non-metallic elements (e.g., nitrogen and phosphorus), so as to develop MW iron-based catalysts with higher catalytic activity and selectivity.

(2) In-depth investigation of the interaction mechanism between MW irradiation and iron-based catalysts. At present, the interaction mechanism between MW and iron-based catalysts is still unclear, and many mechanisms and treatment pathways are mostly speculative; there are controversies about the thermal and non-thermal effects of MW, which limit the further optimization and application of this technology. Therefore, advanced characterization techniques, such as *in situ* Raman spectroscopy, should be used to monitor the structural changes and reaction processes of catalysts under MW irradiation in real time. At the same time, the application of DFT should be further deepened to gain a deeper understanding of the interaction mechanism between MW and catalysts at the atomic and molecular levels.

(3) Optimization of the reaction device. In practical applications, the reactor has a large impact on the performance of the catalyst and the final treatment effect; however, the research on MW reactors is relatively lagging behind compared with the progress made in MW technology. In the future, more investment should be made to develop new types of MW reactors that can be used under different conditions, such as designing reactor lining materials with efficient MW absorption and energy conversion capabilities, optimizing the MW field distribution in the reactor, and improving the utilization of MW energy. At the same time, the scalability and ease of operation of the reactor should be considered so that it can be adapted to different application scenarios from small trials to industrial scale, thus improving the efficiency of pollutant treatment and promoting the industrialization process.

(4) To study the coupling of auxiliary technologies such as photo-radiation, electrochemistry, and plasma with iron-based MW catalytic technology. Although MW radiation itself can significantly improve the processing efficiency of the catalytic system, there is still room for further enhancing the system performance. In future studies, the coupling of iron-based MW catalytic technology with other means can be considered. For example, combining with light irradiation technology to utilize the synergistic effect of photogenerated carriers and MW to enhance the catalyst activity; introducing electrochemical assistance to improve the mass transfer efficiency and reaction rate of pollutants through the modulation effect of electric field; or coupling with plasma technology to utilize the higher electrons and free radicals generated by plasma to further enhance the degradation process of pollutants. Through the combination of multiple technologies, the benefits can be maximized, and the application range and treatment capacity of the technology can be expanded.

(5) Expanding the scope of treatment objects. At present, the research of MW iron-based catalysts is mostly focused on the experimental treatment of organic wastewater, while it is less applied in other important environmental fields such as air purification and solid-waste resource utilization. In the future, the research field should be further expanded to gradually realize practical applications. For example, in the field of air purification, the removal effect of volatile organic compounds and fine particulate matter (PM2.5) should be investigated; and in the field of solid waste recycling, efficient treatment processes should be developed for the recovery of valuable components from solid waste, so as to give full play to the comprehensive environmental benefits of this technology.

(6) Focus on the toxicity evaluation of by-products in the system. Although MW-Fe-based catalysts can achieve high pollutant removal rates under specific conditions, some by-products may have higher toxicity than the original pollutants themselves, which is potentially harmful to the environment. Therefore, the toxicity of the by-products in the system needs to be closely monitored in future studies. Advanced analytical methods, such as LC-HRMS and gas chromatography–mass spectrometry, are used to qualitatively and quantitatively analyze the by-products. At the same time, a comprehensive toxicity evaluation system, including biological toxicity testing and ecological risk assessment, is established to ensure the safety and reliability of the treated environmental media.

Acknowledgments: We are thankful to the National Natural Science Foundation of China, the Guizhou Science and

Technology Plan Project, and the Doctoral Research Fund of Guizhou Normal University for their financial support.

Funding information: This work was financially supported by the National Natural Science Foundation of China (Project No. 22266009); Guizhou Science and Technology Plan Project (Guizhou Science Support [2024] General 103); and Doctoral Research Fund of Guizhou Normal University, China (GZNUD [2019]6).

Author contributions: Ru Li: investigation and roles/ writing – original draft. Sen Li: writing – review and editing and project administration. Yuanhao Wang: investigation and methodology. Hongyi Shen: investigation and resources.

Conflict of interest: The authors state no conflict of interest.

Data availability statement: The datasets generated during and/or analyzed during the current study are available from the corresponding author on reasonable request.

References

[1] Saravanan A, Kumar PS, Hemavathy RV, Jeevanantham S, Harikumar P, Priyanka G, et al. A comprehensive review on sources, analysis and toxicity of environmental pollutants and its removal methods from water environment. Sci Total Environ. 2022;812:152456.

[2] Ismail M, Akhtar K, Khan MI, Kamal T, Khan MA, M Asiri A, et al. Pollution, toxicity and carcinogenicity of organic dyes and their catalytic bio-remediation. Curr Pharm Des. 2019;25(34):3645–63.

[3] Jia Q, Liao GQ, Chen L, Qian YZ, Yan X, Qiu J. Pesticide residues in animal-derived food: Current state and perspectives. Food Chem. 2024;438:137974.

[4] Shan D, Yu H, Yang Z, Li H, Jia R, Zhang Y. Contamination distribution and non-biological removal pathways of typical tetracycline antibiotics in the environment: A review. J Hazard Mater. 2024;463:141308.

[5] Singh N, Ogunseitan OA, Tang Y. Medical waste: Current challenges and future opportunities for sustainable management. Crit Rev Environ Sci Technol. 2021;52(11):2000–22.

[6] Sas OG, Domínguez Á, González B. Recovery and elimination of phenolic pollutants from water using [NTf2] and [Nf2]-based ionic liquids. Appl Sci. 2019;9(20):4321.

[7] Bala S, Garg D, Thirumalesh BV, Sharma M, Sridhar K, Inbaraj BS, et al. Recent strategies for bioremediation of emerging pollutants: a review for a green and sustainable environment. Toxics. 2022;10(8):484.

[8] Sylwan I, Thorin E. Removal of heavy metals during primary treatment of municipal wastewater and possibilities of enhanced removal: a review. Water. 2021;13(8):1121.

[9] Jatoi AS, Hashmi Z, Adriyani R, Yuniarto A, Mazari SA, Akhter F, et al. Recent trends and future challenges of pesticide removal techniques – A comprehensive review. J Environ Chem Eng. 2021;9(4):105571.

[10] Chang N, Liu J, Ji Y, Liu J, Chen Y. Kinetic study of Rhodamine B degradation of electro-catalysis by TiO_2/activated semi-coke composite as tiny electrode. J Sol-Gel Sci Technol. 2023;106(3):684–98.

[11] Lin X, Zhou Q, Xu H, Chen H, Xue G. Advances from conventional to biochar enhanced biotreatment of dyeing wastewater: A critical review. Sci Total Environ. 2024;907:167975.

[12] Pan Y, Zhang Y, Hou M, Xue J, Qin R, Zhou M, et al. Properties of polyphenols and polyphenol-containing wastewaters and their treatment by Fenton/Fenton-like reactions. Sep Purif Technol. 2023;317:123905.

[13] Baharim NH, Sjahrir F, Mohd Taib R, Idris N, Tuan Daud TA. Methylene blue adsorption by acid post-treated low temperature biochar derived from banana (Musa acuminata) pseudo stem. Sains Malaysiana. 2023;52(2):547–61.

[14] Peiris S, de Silva HB, Ranasinghe KN, Bandara SV, Perera IR. Recent development and future prospects ofTiO_2 photocatalysis. J Chin Chem Soc. 2021;68(5):738–69.

[15] Rasouli S, Rezaei N, Hamedi H, Zendehboudi S, Duan X. Superhydrophobic and superoleophilic membranes for oil-water separation application: A comprehensive review. Mater Des. 2021;204:109599.

[16] Jiang Y, Zhao H, Liang J, Yue L, Li T, Luo Y, et al. Anodic oxidation for the degradation of organic pollutants: Anode materials, operating conditions and mechanisms. A mini review. Electrochem Commun. 2021;123:106912.

[17] Ariaeenejad S, Kavousi K, Han JL, Ding XZ, Hosseini Salekdeh G. Efficiency of an alkaline, thermostable, detergent compatible, and organic solvent tolerant lipase with hydrolytic potential in biotreatment of wastewater. Sci Total Environ. 2023;866:161066.

[18] Saravanan A, Kumar PS, Jeevanantham S, Anubha M, Jayashree S. Degradation of toxic agrochemicals and pharmaceutical pollutants: Effective and alternative approaches toward photocatalysis. Environ Pollut. 2022;298:118844.

[19] Chu Z, Zheng L, Lai K. MW microscopy and its applications. Annu Rev Mater Res. 2020;50(1):105–30.

[20] Garcia-Costa AL, Zazo JA, Casas JA. MW-assisted catalytic wet peroxide oxidation: Energy optimization. Sep Purif Technol. 2019;215:62–9.

[21] Feng Y, Tao Y, Meng Q, Qu J, Ma S, Han S, et al. MW-combined advanced oxidation for organic pollutants in the environmental remediation: An overview of influence, mechanism, and prospective. Chem Eng J. 2022;441:135924.

[22] Palma V, Barba D, Cortese M, Martino M, Renda S, Meloni E. MWs and heterogeneous catalysis: a review on selected catalytic processes. Catalysts. 2020;10(2):246.

[23] Gao Y, Liu Y, Zou D. MW-assisted synthesis and environmental remediation: a review. Environ Chem Lett. 2023;21(4):2399–416.

[24] Mishra S, Kumari S, Kumar P, Samanta SK. MW synthesized strontium hexaferrite 2D sheets as versatile and efficient MW catalysts for degradation of organic dyes and antibiotics. Sci Total Environ. 2021;790:147853.

[25] Zhi K, Li Z, Ma P, Tan Y, Zhou Y, Zhang W, et al. A review of activation persulfate by iron-based catalysts for degrading wastewater. Appl Sci. 2021;11(23):11314.

[26] Yuan S, Xue Y, Ma R, Ma Q, Chen Y, Fan J. Advances in iron-based electrocatalysts for nitrate reduction. Sci Total Environ. 2023;866:161444.
[27] Chen B, Shi Y, Li J, Zhai J, Liu L, Liu W, et al. Application of functional modification of iron-based materials in advanced oxidation processes (AOPs). Water. 2022;14(9):2276–85.
[28] Oh SY, Chiu PC, Kim BJ, Cha DK. Enhanced reduction of perchlorate by elemental iron at elevated temperatures. J Hazard Mater. 2006;129(1–3):304–7.
[29] Xu D, Lai X, Guo W, Dai P. MW-assisted catalytic degradation of methyl orange in aqueous solution by ferrihydrite/maghemite nanoparticles. J Water Process Eng. 2017;16:270–6.
[30] Shen M, Fu L, Tang J, Liu M, Song Y, Tian F, et al. MW hydrothermal-assisted preparation of novel spinel-NiFe 2 O 4/ natural mineral composites as MW catalysts for degradation of aquatic organic pollutants. J Hazard Mater. 2018;350:1–9.
[31] Mao Y, Xi Z, Wang W, Ma C, Yue Q. Kinetics of Solvent Blue and Reactive Yellow removal using MW radiation in combination with nanoscale zero-valent iron. J Environ Sci. 2015;30:164–72.
[32] Falciglia PP, Roccaro P, Bonanno L, De Guidi G, Vagliasindi FGA, Romano S. A review on the MW heating as a sustainable technique for environmental remediation/detoxification applications. Renew Sustain Energy Rev. 2018;95:147–70.
[33] Li H, Zhang C, Pang C, Li X, Gao X. The advances in the special MW effects of the heterogeneous catalytic reactions. Front Chem. 2020;8:355.
[34] Xia H, Li C, Yang G, Shi Z, Jin C, He W, et al. A review of MW-assisted advanced oxidation processes for wastewater treatment. Chemosphere. 2022;287:131981.
[35] Asomaning J, Haupt S, Chae M, Bressler DC. Recent developments in MW-assisted thermal conversion of biomass for fuels and chemicals. Renew Sustain Energy Rev. 2018;92:642–57.
[36] Hashim KS, Shaw A, AlKhaddar R, Kot P, Al-Shamma'a A. Water purification from metal ions in the presence of organic matter using electromagnetic radiation-assisted treatment. J Clean Prod. 2021;280:124427.
[37] Horikoshi S, Kajitani M, Serpone N. The MW-/photo-assisted degradation of bisphenol-A in aqueous TiO2 dispersions revisited. J Photochem Photobiol A: Chem. 2007;188(1):1–4.
[38] Yin Y, Wang X, Hu Y, Li F, Cheng H. Cu-Mn-CeOx loaded ceramic catalyst for non-thermal sterilization and MW thermal catalysis of VOCs degradation. Chem Eng J. 2022;442:130063.
[39] <*Thermal and non-thermal effects of MWs in synthesis.pdf*>.
[40] Sahoo BM, Panda J, Banik BK. Thermal and non-thermal effects of MWs in synthesis. J Indian Chem Soc. 2018;95(11):1311–9.
[41] Wang N, Hu Q, Du X, Xu H, Hao L. Study on decolorization of Rhodamine B by raw coal fly ash catalyzed Fenton-like process under MW irradiation. Adv Powder Technol. 2019;30(10):2369–78.
[42] Ren Y, Zhou J, Pan Z, Lai B, Yuan D. Rapid removal of ultra-high-concentration p-nitrophenol in aqueous solution by MW-enhanced Fe/Cu bimetallic particle (MW-Fe/Cu) system. Environ Technol. 2017;40(2):239–49.
[43] Yuan B, Qian Z, Yang X, Luo M, Feng X, Fu L, et al. MW-induced deep catalytic oxidation of NO using molecular-sieve-supported oxygen-vacancy-enriched Fe–Mn bimetal oxides. Environ Sci Technol. 2022;56(14):10423–32.
[44] Cao M, Xu P, Tian K, Shi F, Zheng Q, Ma D, et al. Recent advances in MW-enhanced advanced oxidation processes (MAOPs) for environmental remediation: A review. Chem Eng J. 2023;471:144208.
[45] Chen D, Mei CY, Yao LH, Jin HM, Qian GR, Xu ZP. Flash fixation of heavy metals from two industrial wastes into ferrite by MW hydrothermal co-treatment. J Hazard Mater. 2011;192(3):1675–82.
[46] Gaffar S, Kumar A, Riaz U. Synthesis techniques and advance applications of spinel ferrites: A short review. J Electroceram. 2023;51(4):246–57.
[47] Januskevicius J, Stankeviciute Z, Baltrunas D, Mažeika K, Beganskiene A, Kareiva A. Aqueous sol-gel synthesis of different iron ferrites: From 3D to 2D. Materials. 2021;14(6):1554.
[48] Bharadwaj S, Lakshmi YK, Dhand V, Narayana MV, Rajendrachary M. A brief comparison of structural and magnetic properties of bismuth ferrite prepared using hydrothermal and sol–gel synthesis methods. J Sol-Gel Sci Technol. 2024;109(3):810–6.
[49] Xing L, Shun-kang P, Xing Z, Li-chun C. MW-absorbing properties of strontium ferrites prepared via sol-gel method. Cryst Res Technol. 2017;52(5):1700057.
[50] Qin H, He Y, Xu P, Huang D, Wang Z, Wang H, et al. Spinel ferrites (MFe_2O_4): Synthesis, improvement and catalytic application in environment and energy field. Adv Colloid Interface Sci. 2021;294:102486.
[51] Zhang W, Li X, Zou R, Wu H, Shi H, Yu S, et al. Magnetic nano-sized cadmium ferrite as an efficient catalyst for the degradation of Congo red in the presence of MW irradiation. RSC Adv. 2015;5(63):51027–34.
[52] Zia J, Riyazuddin M, Aazam ES, Riaz U. Rapid catalytic degradation of amoxicillin drug using ZnFe2O4/PCz nanohybrids under MW irradiation. Mater Sci Eng: B. 2020;261:114713.
[53] Luo H, Zeng Y, He D, Pan X. Application of iron-based materials in heterogeneous advanced oxidation processes for wastewater treatment: A review. Chem Eng J. 2021;407:127191.
[54] Xu Q, Yajima T, Li W, Saito K, Ohshima Y, Yoshikai Y. Synthesis, properties, and environmental applications of nanoscale iron-based materials: a review. Crit Rev Environ Sci Technol. 2006;36(5):405–31.
[55] Yirsaw BD, Megharaj M, Chen Z, Naidu R. Environmental application and ecological significance of nano-zero valent iron. J Environ Sci. 2016;44:88–98.
[56] Crane RA, Scott TB. Nanoscale zero-valent iron: Future prospects for an emerging water treatment technology. J Hazard Mater. 2012;211–212:112–25.
[57] Xu Y, Yuan CG. Preparation, stabilization and applications of nano-zero-valent iron composites in water treatment. Prog Chem. 2022;34(3):717–42.
[58] Li X-Q, Elliott DW, Zhang W-X. Zero-valent iron nanoparticles for abatement of environmental pollutants: Materials and engineering aspects. Crit Rev Solid State Mater Sci. 2006;31(4):111–22.
[59] Mukherjee R, Kumar R, Sinha A, Lama Y, Saha AK. A review on synthesis, characterization, and applications of nano zero valent iron (nZVI) for environmental remediation. Crit Rev Environ Sci Technol. 2015;46(5):443–66.
[60] Jou C-J. Degradation of pentachlorophenol with zero-valence iron coupled with MW energy. J Hazard Mater. 2008;152(2):699–702.
[61] Wacławek S, Nosek J, Cádrová L, Antoš V, Černík M. Use of various zero valent irons for degradation of chlorinated ethenes and ethanes. Ecol Chem Eng S. 2015;22(4):577–87.
[62] Lee CL, Jou CJG, Wang HP. Enhanced degradation of chlorobenzene in aqueous solution using MW-induced zero-

valent iron and copper particles. Water Environ Res. 2010;82(7):642–7.
[63] Tang J, Wu Y, Li X, Bu L, Chang B. Single-atom iron catalysts for biomedical applications. Prog Mater Sci. 2022;128:100959.
[64] Gao L, Chen S, Cai R, Zhao Q, Zhao X, Yang D. Single-atom catalysts: Synthetic strategies and electrochemical applications. Joule. 2018;2(7):1242–64.
[65] Zhang W, Fu Q, Luo Q, Sheng L, Yang J. Understanding single-atom catalysis in view of theory. JACS Au. 2021;1(12):2130–45.
[66] Xia W, Lai G, Li Y, Zeng C, Sun C, Zhang P, et al. Preparation, characterization of iron-based single-atom catalysts and its application for photocatalytic degradation of contaminants in water. J Environ Chem Eng. 2023;11(5):1170212.
[67] Yao Y, Yin H, Gao M, Hu Y, Hu H, Yu M, et al. Electronic structure modulation of covalent organic frameworks by single-atom Fe doping for enhanced oxidation of aqueous contaminants. Chem Eng Sci. 2019;209:115211.
[68] Lin L, Chen Z, Chen W. Single atom catalysts by atomic diffusion strategy. Nano Res. 2021;14(12):4398–416.
[69] Zhou Y, Yu Y, Ma D, Foucher AC, Xiong L, Zhang J, et al. Atomic Fe dispersed hierarchical mesoporous Fe–N–C nanostructures for an efficient oxygen reduction reaction. ACS Catal. 2020;11(1):74–81.
[70] Wang Z, Jin X, Zhu C, Liu Y, Tan H, Ku R, et al. Atomically dispersed Co2–N6 and Fe–N4 costructures boost oxygen reduction reaction in both alkaline and acidic media. Adv Mater. 2021;33(49):2104718.
[71] Shang H, Wang T, Pei J, Jiang Z, Zhou D, Wang Y, et al. Design of a single-atom Indiumδ + –N4 interface for efficient electroreduction of CO_2 to formate. Angew Chem Int Ed. 2020;59(50):22465–9.
[72] Shang H, Jiang Z, Zhou D, Pei J, Wang Y, Dong J, et al. Engineering a metal–organic framework derived Mn–N4–CxSy atomic interface for highly efficient oxygen reduction reaction. Chem Sci. 2020;11(23):5994–9.
[73] Zhang X, Shi Y, Xu J, Ouyang Q, Zhang X, Zhu C, et al. Identification of the intrinsic dielectric properties of metal single atoms for electromagnetic wave absorption. Nano-Micro Lett. 2021;14(1).
[74] Zhou C, Sun QM, Cao Q, He JH, Lu JM. Synergistic effect of Fe single-atom catalyst for highly efficient MW-stimulated remediation of chloramphenicol-contaminated soil. Small. 2022;19(2):2205341.
[75] Sun Y, Zheng L, Zheng X, Xiao D, Yang Y, Zhang Z, et al. Effective removal of 2,4,6-trichlorophenol by FeSx/talc composite under MW. J Environ Chem Eng. 2021;9(4):814647.
[76] Liu Z, Zhang W, Liang Q, Huang J, Shao B, Liu Y, et al. MW-assisted high-efficiency degradation of methyl orange by using CuFe2O4/CNT catalysts and insight into degradation mechanism. Environ Sci Pollut Res. 2021;28(31):42683–93.
[77] Liu Y-W, Zhang J, Gu LS, Wang LX, Zhang QT. Preparation and electromagnetic properties of nanosized Co0.5Zn0.5Fe2O4 ferrite. Rare Met. 2016;41(9):3228–32.
[78] Ambika S, Gopinath S, Saravanan K, Sivakumar K, Sukantha TA, Paramasivan P. Preparation and characterization of nanocopper ferrite and its green catalytic activity in alcohol oxidation reaction. J Supercond Nov Magn. 2018;32(4):903–10.
[79] Fu Y, Tang Y, Shi W, Chen F, Guo F, Hao C. Preparation of rambutan-shaped hollow ZnFe2O4 sphere photocatalyst for the degradation of tetracycline by visible-light photocatalytic persulfate activation. Mater Chem Phys. 2022;286:126176.
[80] Xu Z, Fan J, Han Y, Liu T, Zhang H, Song K, et al. Preparation and characterization of Mn–Zn ferrites via nano-in-situ composite method. Solid State Sci. 2019;98:106006.
[81] Sarkar P, De S, Neogi S. MW assisted facile fabrication of dual Z-scheme g-C3N/ZnFe2O4/Bi2S3 photocatalyst for peroxymonosulphate mediated degradation of 2,4,6-Trichlorophenol: The mechanistic insights. Appl Catal B: Environ. 2022;307:121165.
[82] Zhang B, Wang D. Preparation of biomass activated carbon supported nanoscale zero-valent iron (Nzvi) and its application in decolorization of methyl orange from aqueous solution. Water. 2019;11(8):1671.
[83] Sun G, Zhang J, Meng W, Wang L. Optimization of preparation of montmorillonite nanometer zero-valent iron and the degradation of amoxicillin by response surface methodology. Water Supply. 2020;20(8):3625–35.
[84] Shekarriz M, Ramezani Z, Elhami F. Preparation and characterization of ZSM5-supported nano-zero-valent iron and its potential application in nitrate remediation from aqueous solution. Int J Environ Sci Technol. 2017;14(5):1081–90.
[85] Molla A, Kim AY, Woo JC, Cho HS, Youk JH. Study on preparation methodology of zero-valent iron decorated on graphene oxide for highly efficient sonocatalytic dye degradation. J Environ Chem Eng. 2022;10(2):107214.
[86] Wang K, Wang G, Zhou L, Zeng Y, Zhang Y, Fang Z. Rapid removal of decabromodiphenyl ether by mechanochemically prepared submicron zero-valent iron with FeC2O4·2 H2O layers: Kinetics, mechanisms and pathways. J Hazard Mater. 2024;465:133309.
[87] Shi B, Li H, Fu X, Zhao C, Li M, Liu M, et al. Fe single-atom catalyst for cost-effective yet highly efficient heterogeneous fenton catalysis. ACS Appl Mater Interfaces. 2022;14(48):53767–76.
[88] Zhang W-D, Dong H, Zhou L, Xu H, Wang HR, Yan X, et al. Fe single-atom catalysts with pre-organized coordination structure for efficient electrochemical nitrate reduction to ammonia. Appl Catal B: Environ. 2022;317:121750.
[89] Luo J, Gong G, Ma R, Sun S, Cui C, Cui H, et al. Study on high-value products of waste plastics from MW catalytic pyrolysis: Construction and performance evaluation of advanced MW absorption-catalytic bifunctional catalysts. Fuel. 2023;346:128296.
[90] Wei R, Wang P, Zhang G, Wang N, Zheng T. MW-responsive catalysts for wastewater treatment: A review. Chem Eng J. 2020;382:122781.
[91] Wang J, Tang J. Fe-based Fenton-like catalysts for water treatment: Preparation, characterization and modification. Chemosphere. 2021;276:130177.
[92] Shao L, Zhang W, Armbrüster M, Teschner D, Girgsdies F, Zhang B, et al. Nanosizing intermetallic compounds onto carbon nanotubes: Active and selective hydrogenation catalysts. Angew Chem Int Ed. 2011;50(43):10231–5.
[93] Zhang B, Li Y, Lu S, Hu Y, Li Y, Wang S, et al. Co-, Ni-, and Cu-doped Fe-based catalysts for the MW-assisted catalytic pyrolysis of polyethylene. ChemSusChem. 2024;17(7):e202301563.
[94] Elías V, Sathicq AG, Cuello N, Luque R, Elsharif AM, Tolley A, et al. Design of Fe-modified mesoporous nanostructures as efficient catalysts for MW-assisted selective oxidations of sulfides. Appl Catal A: Gen. 2021;615:118027.
[95] Lounnas A, Moumen A, Zouaoui E, Belhocine Y, Sobhi C, Rahali S, et al. Degradation by photo-Fenton process using Fe-clay as heterogeneous catalyst under sunlight and MW irradiation. Inorg Chem Commun. 2024;168:112965.

[96] Khan H, Yerramilli AS, D'Oliveira A, Alford TL, Boffito DC, Patience GS. Experimental methods in chemical engineering: X-ray diffraction spectroscopy – XRD. Can J Chem Eng. 2020;98(6):1255–66.
[97] Roshani R, Tadjarodi A. Synthesis of $ZnFe_2O_4$ nanoparticles with high specific surface area for high-performance supercapacitor. J Mater Sci: Mater Electron. 2020;31(24):23025–36.
[98] Jambhulkar DK, Ugwekar RP, Bhanvase BA, Barai DP. A review on solid base heterogeneous catalysts: preparation, characterization and applications. Chem Eng Commun. 2020;209(4):433–84.
[99] Tantuvoy S, Bose S, Ghosh A, Kumar S, Kumar M. MW catalytic treatment using magnetically separable CoFe2O4 spinel catalyst for high-rate degradation of malachite green dye. J Environ Manag. 2025;373:123772.
[100] Isaacs MA, Davies-Jones J, Davies PR, Guan S, Lee R, Morgan DJ, et al. Advanced XPS characterization: XPS-based multi-technique analyses for comprehensive understanding of functional materials. Mater Chem Front. 2021;5(22):7931–63.
[101] Zhou W, Yu Y, Xiong X, Zhou S. Fabrication of α-Fe/Fe3C/ Woodceramic Nanocomposite with Its Improved MW Absorption and Mechanical Properties. Materials. 2018;11(6):878.
[102] Gao J, Yang S, Li N, Meng L, Wang F, He H, et al. Rapid degradation of azo dye Direct Black BN by magnetic $MgFe_2O_4$-SiC under MW radiation. Appl Surf Sci. 2016;379:140–9.
[103] Liu X, Yu J, Cui C, Sun Y, Li X, Li Z. Flower-like BiOI microsphere/ Ni@ C nanocapsule hybrid composites and their efficient MW absorbing activity. J Phys D: Appl Phys. 2018;51(26):265002.
[104] Gao Y, Cong S, Yu H, Zou D. Investigation on MW absorbing properties of 3D C@ZnCo2O4 as a highly active heterogenous catalyst and the degradation of ciprofloxacin by activated persulfate process. Sep Purif Technol. 2021;262:118330.
[105] Peymanfar R, Norouzi F, Javanshir S. Preparation and characterization of one-pot PANi/Fe/Fe3O4/Fe2O3 nanocomposite and investigation of its MW, magnetic and optical performance. Synth Met. 2019;252:40–9.
[106] Gao Y, Wang W, Xu M, Hao Y, Zou D. The magnetically recoverable C-$ZnFe_2O_4$ as a MW absorption catalyst for the degradation of norfloxacin by persulfate: Mechanism, degradation pathway, toxicity, and stability. J Environ Chem Eng. 2022;10(3):107434.
[107] Barham JP, Koyama E, Norikane Y, Ohneda N, Yoshimura T. MW Flow: A perspective on reactor and MW configurations and the emergence of tunable single-mode heating toward large-scale applications. Chem Rec. 2018;19(1):188–203.
[108] Dąbrowska S, Chudoba T, Wojnarowicz J, Łojkowski W. Current trends in the development of MW reactors for the synthesis of nanomaterials in laboratories and industries: a review. Crystals. 2018;8(10):379.
[109] Goyal H. Process intensification using MW heated multiphase reactors. Chem Eng Process - Process Intensif. 2022;178:109026.
[110] Tripathy BK, Kumar M. Suitability of MW and MW-coupled systems for landfill leachate treatment: An overview. J Environ Chem Eng. 2017;5(6):6165–78.
[111] Sauks JM, Mallik D, Lawryshyn Y, Bender T, Organ M. A continuous-flow MW reactor for conducting high-temperature and high-pressure chemical reactions. Org Process Res Dev. 2014;18(11):1310–4.
[112] Xue C, Mao Y, Wang W, Song Z, Zhao X, Sun J, et al. Current status of applying MW-associated catalysis for the degradation of organics in aqueous phase – A review. J Environ Sci. 2019;81:119–35.
[113] Kappe CO. Controlled MW heating in modern organic synthesis. Angew Chem Int Ed. 2004;43(46):6250–84.
[114] Wang A, Zhang Y, Zhong H, Chen Y, Tian X, Li D, et al. Efficient mineralization of antibiotic ciprofloxacin in acid aqueous medium by a novel photoelectro-Fenton process using a MW discharge electrodeless lamp irradiation. J Hazard Mater. 2018;342:364–74.
[115] Zhang Q, Sun Y, Xu W, Cao Y, Wu C, Wang CH, et al. Efficient MW-assisted mineralization of oxytetracycline driven by persulfate and hypochlorite over Cu-biochar catalyst. Bioresour Technol. 2023;372:128698.
[116] Li S, Pang J, Han W, Cheng X, Meng C, Li N, et al. Co nanoparticles/ N-doped carbon nanotubes hybrids as highly efficient catalysts for MW-induced catalytic degradation of tetracycline. J Environ Chem Eng. 2023;11(1):109274.
[117] Rana KK, Rana S. MW reactors: A brief review on its fundamental aspects and applications. Open Access Library J. 2014;1(6):1–20.
[118] Chen W, Malhotra A, Yu K, Zheng W, Plaza-Gonzalez PJ, Catala-Civera JM, et al. Intensified MW-assisted heterogeneous catalytic reactors for sustainable chemical manufacturing. Chem Eng J. 2021;420:130476.
[119] Yan P, Stankiewicz AI, Eghbal Sarabi F, Nigar H. MW heating in heterogeneous catalysis: Modelling and design of rectangular traveling-wave MW reactor. Chem Eng Sci. 2021;232:116383.
[120] Godwin DR, Lawton SJ, Moseley JD, Welham MJ, Weston NP. Energy efficiency of conventionally-heated pilot plant reactors compared with MW reactors. Energy Fuels. 2010;24(10):5446–53.
[121] Wang W, Zhao C, Sun J, Wang X, Zhao X, Mao Y, et al. Quantitative measurement of energy utilization efficiency and study of influence factors in typical MW heating process. Energy. 2015;87:678–85.
[122] Shen T, Tian K, Cao M, Li L, Shi F, Qu J, et al. Application of nickel foam supported Cu–MnO_2 in MW enhanced Fenton-like process for p-nitrophenol removal: Degradation, synergy and mechanism insight. J Clean Prod. 2023;397:136442.
[123] Zhang W, Huang T, Ren Y, Yang S, Zhao X, Yuan M, et al. A multifunctional chitosan composite aerogel for PPCPs adsorption. Carbohydr Polym. 2022;298:120102.
[124] Xu J, Zhang Z, Yang J, Ma Y, Han T, Quan G, et al. Treatment of pharmaceuticals and personal care products (PPCPs) using periodate-based advanced oxidation technology: A review. Chem Eng J. 2025;512:162355.
[125] Vieira Y, Severo de Carvalho G, Leichtweis J, Mistura CM, Foletto EL, Nawaz A, et al. CuFeS2/activated carbon heterostructure as a MW-responsive catalyst for reductive and oxidative degradation of ibuprofen, ketoprofen, and diclofenac. Chem Eng J. 2024;480:148060.
[126] Zia J, Farhat SM, Aazam ES, Riaz U. Highly efficient degradation of metronidazole drug using $CaFe_2O_4$/PNA nanohybrids as metal-organic catalysts under MW irradiation. Environ Sci Pollut Res. 2020;28(4):4125–35.
[127] Saputera WH, Putrie AS, Esmailpour AA, Sasongko D, Suendo V, Mukti RR. Technology advances in phenol removals: Current progress and future perspectives. Catalysts. 2021;11(8):998.
[128] Wang H, Zhang D, Zhao Y, Xie M. Cationic surfactant modified attapulgite for removal of phenol from wastewater. Colloids Surf A: Physicochem Eng Asp. 2022;641:128479.
[129] Rafiq A, Ikram M, Ali S, Niaz F, Khan M, Khan Q, et al. Photocatalytic degradation of dyes using semiconductor photocatalysts to clean industrial water pollution. J Ind Eng Chem. 2021;97:111–28.

[130] Shi Y, Yang Z, Xing L, Zhang X, Li X, Zhang D. Recent advances in the biodegradation of azo dyes. World J Microbiol Biotechnol. 2021;37(8):137.
[131] Zeng Q, Wang Y, Zan F, Khanal SK, Hao T. Biogenic sulfide for azo dye decolorization from textile dyeing wastewater. Chemosphere. 2021;283:131158.
[132] Saha P, Bhaskara Rao KV. Immobilization as a powerful bioremediation tool for abatement of dye pollution: a review. Environ Rev. 2021;29(2):277–99.
[133] Mao Y, Xu J, Ma C. A continuous MW/nZVI treatment system for malachite green removal: system setup and parameter optimization. Desalin Water Treat. 2016;57(51):24395–405.
[134] Wang G, Yang L, Jiang L, Chen J, Jing Q, Mai Y, et al. Overview assessment of risk evaluation and treatment technologies for heavy metal pollution of water and soil. J Clean Prod. 2022;379:134632.
[135] Li Q, Zhang Y, Yu L, Cao K, Si M, Liao Q, et al. Performance and mechanisms of MW-assisted zerovalent iron/pyrite for advance remediation of strongly alkaline high Cr(VI) contaminated soil. Environ Pollut. 2022;298:118855.
[136] Li S, Wu Y, Zheng H, Zheng Y, Jing T, Tian J, et al. High MW responsivity Co–Bi25FeO40 in synergistic activation of peroxydisulfate for high efficiency pollutants degradation and disinfection: Mechanism of enhanced electron transfer. Chemosphere. 2022;288:132558.
[137] Fadaei A. Comparison of medical waste management methods in different countries: a systematic review. Rev Environ Health. 2023;38(2):339–48.
[138] Erdogan AA, Yilmazoglu MZ. Experimental and numerical investigation of medical waste disposal via plasma gasification. Appl Energy. 2024;353:122014.
[139] Yuwen C, Liu B, Rong Q, Hou K, Zhang L, Guo S. Mechanism of MW-assisted iron-based catalyst pyrolysis of discarded COVID-19 masks. Waste Manag. 2023;155:77–86.
[140] Remya N, Lin J-G. MW-assisted carbofuran degradation in the presence of GAC, ZVI and H2O2: Influence of reaction temperature and pH. Sep Purif Technol. 2011;76(3):244–52.
[141] Wang Y, Wang R, Lin N, Wang Y, Zhang X. Highly efficient MW-assisted Fenton degradation bisphenol A using iron oxide modified double perovskite intercalated montmorillonite composite nanomaterial as catalyst. J Colloid Interface Sci. 2021;594:446–59.
[142] Mishra S, Sahu TK, Verma P, Kumar P, Samanta SK. MW-assisted catalytic degradation of brilliant green by spinel zinc ferrite sheets. ACS Omega. 2019;4(6):10411–8.
[143] Hu L, Wang P, Liu G, Zheng Q, Zhang G. Catalytic degradation of p-nitrophenol by magnetically recoverable Fe3O4 as a persulfate activator under MW irradiation. Chemosphere. 2020;240:124977.
[144] Wu D, Kan H, Zhang Y, Wang T, Qu G, Zhang P, et al. Pyrene contaminated soil remediation using MW/magnetite activated persulfate oxidation. Chemosphere. 2022;286:131787.
[145] Gao Y, Cong S, He Y, Zou D, Liu Y, Yao B, et al. Study on the mechanism of degradation of tetracycline hydrochloride by MW-activated sodium persulfate. Water Sci Technol. 2020;82(9):1961–70.
[146] Zhang Z, Shan Y, Wang J, Ling H, Zang S, Gao W, et al. Investigation on the rapid degradation of congo red catalyzed by activated carbon powder under MW irradiation. J Hazard Mater. 2007;147(1–2):325–33.
[147] Shah NS, He X, Khan HM, Khan JA, O'Shea KE, Boccelli DL, et al. Efficient removal of endosulfan from aqueous solution by UV-C/peroxides: A comparative study. J Hazard Mater. 2013;263:584–92.
[148] Gogoi D, Karmur RS, Das MR, Ghosh NN. Cu and $CoFe_2O_4$ nanoparticles decorated hierarchical porous carbon: An excellent catalyst for reduction of nitroaromatics and MW-assisted antibiotic degradation. Appl Catal B: Environ. 2022;312:121407.
[149] Remya N, Lin J-G. Current status of MW application in wastewater treatment – A review. Chem Eng J. 2011;166(3):797–813.
[150] Moradi SE, Dadfarnia S, Haji Shabani AM, Emami S. MW-enhanced Fenton-like degradation by surface-modified metal–organic frameworks as a promising method for removal of dye from aqueous samples. Turkish J Chem. 2017;41:426–39.
[151] He Z, Tian Z, Luo J, Sun S, Zhu G, Ma R. Enhanced peroxymonosulfate activation for degradation of iodinated contrast media by MW-induced bimetallic carbon-based catalysts: Insight into the synergistic mechanism between MWs and bimetallic sites. Chem Eng J. 2024;488:151061.
[152] Tang C, Zhu Y, Liang Y, Zeng YH, Peng X, Mai BX, et al. First discovery of iodinated polyfluoroalkyl acids by nontarget mass-spectrometric analysis and iodine-specific screening algorithm. Environ Sci Technol. 2023;57(3):1378–90.
[153] Gajewicz-Skretna A, Wyrzykowska E, Gromelski M. Quantitative multi-species toxicity modeling: Does a multi-species, machine learning model provide better performance than a single-species model for the evaluation of acute aquatic toxicity by organic pollutants? Sci Total Environ. 2023;861:160590.
[154] Meng Y, Huang H, Zhang Y, Cao Y, Lu H, Li X. Recent advances in the theoretical studies on the electrocatalytic CO_2 reduction based on single and double atoms. Front Chem. 2023;11:1172146.
[155] Fang X-T, Zhou L, Chen C, Danilov DL, Qiao F, Li H, et al. Theoretical calculations facilitating catalysis for advanced lithium-sulfur batteries. Molecules. 2023;28(21):7304.
[156] Wang Y, Wang R, Lin N, Xu J, Liu X, Liu N, et al. Degradation of norfloxacin by MOF-derived lamellar carbon nanocomposites based on MW-driven Fenton reaction: Improved Fe(III)/Fe(II) cycle. Chemosphere. 2022;293:133614.
[157] Grimme S, Antony J, Ehrlich S, Krieg H. A consistent and accurateab initioparametrization of density functional dispersion correction (DFT-D) for the 94 elements H-Pu. The. J Chem Phys. 2010;132(15):154104.
[158] Liu F, Zhu G, Yang D, Jia D, Jin F, Wang W. Systematic exploration of N, C configurational effects on the ORR performance of Fe–N doped graphene catalysts based on DFT calculations. RSC Adv. 2019;9(39):22656–67.
[159] Nørskov JK, Abild-Pedersen F, Studt F, Bligaard T. Density functional theory in surface chemistry and catalysis. Proc Natl Acad Sci. 2011;108(3):937–43.
[160] Mardirossian N, Head-Gordon M. Thirty years of density functional theory in computational chemistry: an overview and extensive assessment of 200 density functionals. Mol Phys. 2017;115(19):2315–72.
[161] Zarpellon J, Mosca DH, Varalda J. Ferromagnetism in heavily Fe-doped GaAs: a DFT study. Phys Scr. 2024;99(9):095998.
[162] Pan J, Liu Y, Lin Q, Deng Y, Luo Y, Zhao Z, et al. Reducing the molecular oxygen activation energy barrier by increasing Fe-O bonds to eliminate antibiotics and their resistance genes. J Hazard Mater. 2025;486:137008.
[163] Yuan G, Li K, Zhang J, Huang Z, Li F, Zhang H, et al. A novel insight into the MW induced catalytic reduction mechanism in aqueous

Cr(VI) removal over $ZnFe_2O_4$ catalyst. J Hazard Mater. 2023;443:130211.
[164] Zhang S, Qin Y, Ding S, Su Y. A DFT study on the activity origin of Fe-N-C sites for oxygen reduction reaction. ChemPhysChem. 2022;23(15):e202200165.
[165] Tang LF, Chen XL, Tao XX. Non-thermal effect of MW on organic sulfur removal from coal by MW with peroxyacetic acid. Fuel. 2023;338:127262.
[166] Tao Y, Yan B, Zhang N, Zhao J, Zhang H, Chen W, et al. Decoupling thermal effects and possible non-thermal effects of MWs in vacuum evaporation of glucose solutions. J Food Eng. 2023;338:111257.
[167] Patil NN, Shukla SR. Degradation of reactive yellow 145 dye by persulfate using MW and conventional heating. J Water Process Eng. 2015;7:314–27.
[168] Wang, X, Jiang L, Li K, Wang J, Fang D, Zhang Y, et al. Fabrication of novel Z-scheme $SrTiO_3/MnFe_2O_4$ system with double-response activity for simultaneous MW-induced and photocatalytic degradation of tetracycline and mechanism insight. Chem Eng J. 2020;400:125981.